# Klamath River, California and Oregon

## Topobathymetric LiDAR and Imagery Technical Data Report

**Contract No. G16PC00016, Task Order 140G0218F0247**

*Prepared For:*

**Leslie Lansbery**
USGS NGTOC
1400 Independence Rd.
Rolla, MO, 65401
PH: 573-308-3538

*Prepared By:*

**QSI Corvallis**
1100 NE Circle Blvd, Ste. 126
Corvallis, OR 97330
PH: 541-752-1204

# TABLE OF CONTENTS

**Cover Photo:** A view of the Klamath River near Stanshaw Creek in California. The image is composed of the gridded topobathymetric model and above ground lidar point cloud colored by elevation.

This photo taken by QSI acquisition staff shows a view of the Klamath River just north of the Salmon River confluence.

In June 2018, Quantum Spatial (QSI) was contracted by the United States Geological Survey (USGS), to collect topobathymetric lidar data and digital imagery in the early summer of 2018 for the Klamath River in California and Oregon (contract no. G16PC00016, task order 140G0218F0247). The Klamath River project encompasses the Klamath River corridor AOI, an area of interconnected reservoirs known as Klamath Reservoirs AOI, and several Klamath River tributaries across south central Oregon and northern California. Conventional near-infrared (NIR) lidar was fully integrated with green wavelength (bathymetric) lidar and sonar depth measurements in order to provide a seamless topobathymetric surface dataset. With authorization from the Klamath River Renewal Corporation (KRRC), multibeam and sweep sonar survey data collected by GMA Hydrology, Inc. (GMA), under contract with AECOM Technical Services, Inc. (AECOM), were provided to QSI for the Klamath Reservoirs AOI. Sonar depth measurements taken within the Klamath Reservoirs AOI were incorporated into the lidar dataset to supplement bathymetric bottom returns in areas too deep for lidar mapping. Data were collected to aid USGS in assessing the channel morphology and topobathymetric surface of the study area as part of a comprehensive characterization of the Klamath River prior to dam removal.

This report accompanies the delivered integrated topobathymetric data and imagery, and documents contract specifications, data acquisition procedures, processing methods, sonar integration, and analysis of the final dataset including lidar accuracy, depth penetration, and density. Acquisition dates and acreage are shown in Table 1, a complete list of contracted deliverables provided to USGS is shown in Table 2, and the project extent is shown in Figure 1. Detailed information specific to sonar acquisition, processing, and analysis may be found in the GMA *2018 Klamath Dam Removal Project: Topobathymetric LiDAR & Sonar Technical Data Report,* included as Appendix B.

**Table 1: Acquisition dates, acreage, and data types collected on the Klamath River project area**

| Project Site | Contracted Acres | Buffered Acres | Acquisition Dates | Data Type |
|---|---|---|---|---|
| **Klamath Reservoirs AOI** | 23,620 | 26,732 | 06/11/2018 – 6/13/2018 | Topobathymetric lidar |
| | | | 6/8/2018 | 4 band (RGB-NIR) Digital Imagery |
| **\*Klamath Reservoirs AOI** | 8.15 | N/A | 2/8/2018 – 8/8/2018<br>5/9/2018 – 5/10/2018<br>5/29/2018 – 5/30/2018 | Multibeam Sonar<br>Sweep Sonar |
| **Klamath River Corridor AOI** | 40,908 | 46,004 | 6/1/2018 – 6/8/2018<br>6/10/2018 – 6/14/2018 | Topobathymetric lidar |
| | | | 6/8/2018 – 6/23/2018 | 4 band (RGB-NIR) Digital Imagery |

*\*Acquired by GMA*



*This photo taken by QSI's acquisition team shows an oblique aerial view of the Klamath River and Iron Gate Dam, taken from the helicopter during lidar flights.*

# Deliverable Products

**Table 2: Products delivered to USGS for the Klamath River sites**

| Klamath River Lidar Products<br>Projection: UTM Zone 10 North<br>Horizontal Datum: NAD83 (2011)<br>Vertical Datum: NAVD88 (GEOID12B)<br>Units: Meters | |
|---|---|
| **Topobathymetric Lidar** | |
| **Points** | LAS v 1.4 PDRF 6<br>• All Classified Returns<br>• Unclassified Flightline Swaths<br>LAS v 1.4 PDRF9<br>• Uncalibrated Flightline Swaths<br>• Waveform data (*.wdp) |
| **Rasters** | 1.0 Meter ERDAS Imagine Files (*.img)<br>• Hydroflattened Bare Earth Digital Elevation Model (DEM)<br>• Topobathymetric Bare Earth Digital Elevation Model (DEM) Clipped<br>• Topobathymetric Bare Earth Digital Elevation Model (DEM) Unclipped<br>• Highest Hit Digital Surface Model (DSM)<br>• Point Density of All Valid Classes<br>0.5 Meter GeoTiffs<br>• Green Sensor Intensity Images<br>• NIR Sensor Intensity Images |
| **Vectors** | Shapefiles (*.shp)<br>• Site Boundary<br>• Tile Index (500m x 500m)<br>• Hydroflattened Breaklines<br>• Water's Edge/Refraction Breaklines<br>• Bathymetric Coverage<br>ESRI File Geodatabase<br>• Flightline Indices<br>• LiDAR Flightline Swath Polygons<br>• Contours (30 cm)<br>Ground Survey Shapefiles (*.shp)<br>• Non-Vegetated Ground Check Points<br>• Vegetated Ground Check Points<br>• Ground Control Points<br>• Ground Control Base Station Coordinates<br>• Bathymetric Check Points<br>• Wetted Edge Check Points<br>• Aerial Targets |
| **4 Band (RGB-NIR) Digital Imagery** | |
| **Digital Imagery** | 15 cm GeoTiffs<br>• Imagery Mosaics (RGB-NIR) |

**Figure 1: Location map of the Klamath River site in California and Oregon**

Klamath Reservoirs AOI
(26,732 acres)

Klamath River AOI
(72,030 acres)

QSI's Bell 206L-3 Rotorcraft

## Planning

In preparation for data collection, QSI reviewed the project area and developed a specialized flight plan to ensure complete coverage of the Klamath River lidar study area at the target combined point density of ≥8 points/m$^2$ for topographic lidar and $\geq 2$ pulses/m$^2$ for submerged topobathymetric lidar. Acquisition parameters including orientation relative to terrain, flight altitude, pulse rate, scan angle, and ground speed were adapted to optimize flight paths and flight times while meeting all contract specifications. QSI's Bell 206L-3 Rotorcraft helicopter was selected for acquisition, allowing for a lower flight AGL and increased maneuverability to navigate the narrow Klamath River corridor which passes through the steep terrain of the Pacific Coast Ranges. Due to the lower flight AGL and slower flight speed of the helicopter, LiDAR point density results were expected to be significantly higher than the contracted density requirements.

Factors such as satellite constellation availability and weather windows must be considered during the planning stage. Any weather hazards or conditions affecting the flight were continuously monitored due to their potential impact on the daily success of airborne and ground operations. In addition, logistical considerations including private property access, potential air space restrictions, channel flow rates, and water clarity (Figure 2 and Table 3) were reviewed.
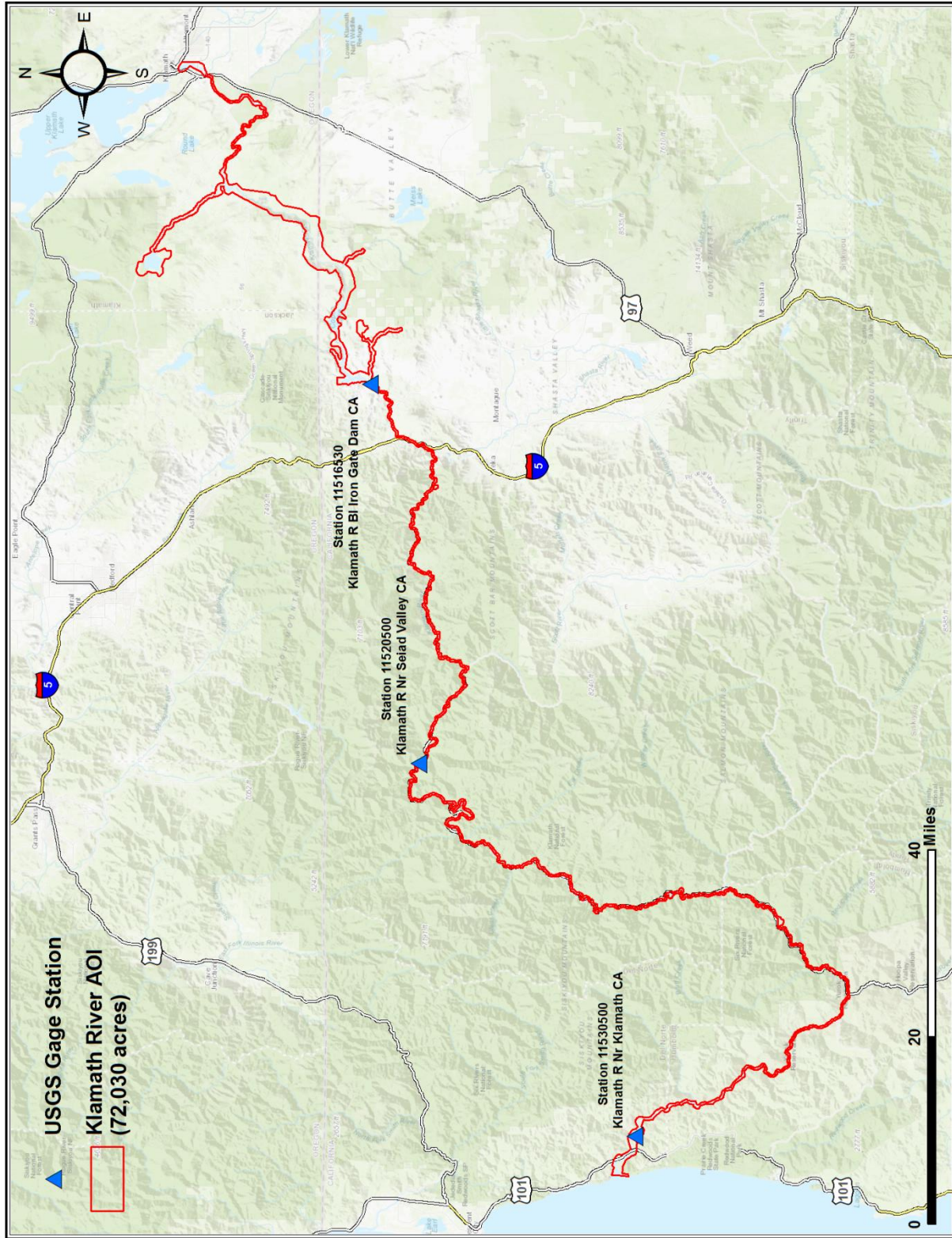
**Figure 2: Selected USGS Gage Station locations within the Klamath River site for review of hydrologic conditions at the time of lidar acquisition**

**Table 3: Hydrologic Conditions for USGS Gage Stations within the Klamath River AOI**

| | USGS Gage Station Daily Average Discharge and Gage Height | | | | | |
|---|---|---|---|---|---|---|
| | USGS Gage Station ID | | | | | |
| | 11516530 | | 11520500 | | 11530500 | |
| Date | Discharge (cfs) | Gage Height (ft) | Discharge (cfs) | Gage Height (ft) | Discharge (cfs) | Gage Height (ft) |
| 6/1/2018 | 1111.04 | 2.28 | 1917.19 | 3.06 | 8606.98 | 10.58 |
| 6/2/2018 | 1030.42 | 2.14 | 1781.56 | 2.90 | 8269.38 | 10.47 |
| 6/3/2018 | 1015.73 | 2.12 | 1696.88 | 2.79 | 7871.25 | 10.33 |
| 6/4/2018 | 992.69 | 2.08 | 1632.53 | 2.71 | 7529.79 | 10.22 |
| 6/5/2018 | 1004.69 | 2.10 | 1607.71 | 2.68 | 7271.60 | 10.13 |
| 6/6/2018 | 1010.10 | 2.10 | 1568.65 | 2.63 | 7023.02 | 10.04 |
| 6/7/2018 | 1227.81 | 2.47 | 1533.33 | 2.58 | 6900.83 | 10.00 |
| 6/8/2018 | 1590.42 | 3.04 | 1852.81 | 2.98 | 6923.96 | 10.01 |
| 6/9/2018 | 1671.25 | 3.16 | 2223.23 | 3.39 | 7235.21 | 10.12 |
| 6/10/2018 | 1547.29 | 2.98 | 2148.02 | 3.32 | 7685.31 | 10.27 |
| 6/11/2018 | 1419.90 | 2.79 | 1993.23 | 3.14 | 7413.23 | 10.18 |
| 6/12/2018 | 1298.13 | 2.60 | 1859.58 | 2.99 | 6905.52 | 10.00 |
| 6/13/2018 | 1228.13 | 2.49 | 1712.19 | 2.81 | 6468.85 | 9.84 |
| 6/14/2018 | 1164.38 | 2.38 | 1645.47 | 2.73 | 6123.96 | 9.72 |

# Turbidity Measurements

In order to assess water clarity conditions prior to and during lidar and digital imagery collection, QSI collected turbidity measurements. Readings were collected at 21 locations throughout the project site between May 31st and June 10th, 2018 Hach 2100Q Turbidimeter.  Each day the Hach sensor is calibrated using 4 precise, pre-mixed calibration standards at 10 NTU, 20 NTU, 100 NTU, and 800 NTU. Turbidity observations were recorded three times to confirm measurements.  The table below provides turbidity results per location in the Klamath River site.



**Figure 3: Hach 2100Q Turbidimeter**

**Table 4: Turbidity Observations**

| Turbidity Measurements | | | | | |
|---|---|---|---|---|---|
| Date | Latitude | Longitude | Turbidity Read 1 | Turbidity Read 2 | Turbidity Read 3 |
| 31-May | 42.218572 | -121.787999 | 5.49 | 4.97 | 5.09 |
| 1-Jun | 42.218725 | -121.788300 | 5.48 | 4.55 | 4.77 |
| 1-Jun | 42.147049 | -121.848249 | 3.67 | 3.78 | 3.5 |
| 2-Jun | 42.135886 | -121.942486 | 6.68 | 6.42 | 6.55 |
| 2-Jun | 42.156311 | -122.027328 | 1.47 | 1.46 | 1.49 |
| 2-Jun | 42.194784 | -122.074742 | 1.34 | 1.57 | 1.94 |
| 3-Jun | 41.899321 | -122.508062 | 3.69 | 3.02 | 3.21 |

| | | | | | |
|---|---|---|---|---|---|
| 3-Jun | 41.930857 | -122.442271 | 3.46 | 3.02 | 3.54 |
| 4-Jun | 41.858400 | -122.750262 | 3.03 | 2.97 | 2.76 |
| 4-Jun | 41.823159 | -122.961854 | 2.71 | 2.71 | 2.54 |
| 4-Jun | 41.778788 | -123.036589 | 2.21 | 2.56 | 2.01 |
| 5-Jun | 41.860133 | -123.307115 | 2.35 | 2.37 | 2.06 |
| 5-Jun | 41.789664 | -123.379247 | 1.06 | 1.01 | 1.88 |
| 5-Jun | 41.669281 | -123.435820 | 2.03 | 1.99 | 1.64 |
| 6-Jun | 41.613580 | -123.495575 | 1.91 | 1.97 | 2.03 |
| 6-Jun | 41.377069 | -123.493623 | 1.29 | 1.52 | 1.23 |
| 7-Jun | 41.251671 | -123.634851 | 1.46 | 1.07 | 1.01 |
| 7-Jun | 41.187766 | -123.712692 | 0.95 | 0.96 | 0.94 |
| 7-Jun | 41.342870 | -123.856264 | 0.74 | 0.95 | 0.85 |
| 8-Jun | 41.515948 | -124.000319 | 1.46 | 1.98 | 1.39 |
| 10-Jun | 41.545343 | -124.070593 | 2.79 | 2.51 | 2.75 |



```
DIRECTION          41°11.268'N          ACCURACY 5 m
280 deg(T)         123°42.766'W         DATUM WGS84




BA007                                   2018-06-07
                                        12:41:48-07:00
```

*These photos taken by QSI acquisition staff display water clarity conditions in the Klamath River during the time of lidar acquisition. The photo above was taken in the Klamath River shallows near Weitchpec, California and the bottom photo was taken near Midland, Oregon in the Klamath River.*

# Airborne Survey

## Lidar

The lidar survey was accomplished using a Riegl VQ-880-G green laser system mounted in a Bell 206L-3 Rotorcraft. The Riegl VQ-880-G uses a green wavelength ($\Lambda$=532 nm) laser that is capable of collecting high resolution vegetation and topography data, as well as penetrating the water surface with minimal spectral absorption by water. The Riegl VQ-880-G contains an integrated NIR laser ($\Lambda$=1064 nm) that adds additional topography data and aids in water surface modeling. The recorded waveform enables range measurements for all discernible targets for a given pulse. The typical number of returns digitized from a single pulse range from 1 to 7 for the Klamath River project area. It is not uncommon for some types of surfaces (e.g., dense vegetation or water) to return fewer pulses to the lidar sensor than the laser originally emitted. The discrepancy between first return and overall delivered density will vary depending on terrain, land cover, and the prevalence of water bodies. All discernible laser returns were processed for the output dataset. Table 5 summarizes the settings used to yield an average pulse density of $\geq$8 pulses/m$^2$ for topographic lidar and $\geq$2 pulses/m$^2$ for submerged topobathymetric lidar over the Klamath River project area.

**Table 5: Lidar specifications and survey settings**

| Lidar Survey Settings & Specifications | | |
|---|---|---|
| Acquisition Dates | June 1 - 8, 2018 June 10 - 14, 2018 | |
| Aircraft Used | Bell 206L-3 Rotorcraft | |
| Sensor | Riegl | |
| Laser | VQ-880-G | VQ-880-G-IR |
| Maximum Returns | 15 | 15 |
| Resolution/Density (Topographic) | Average 8 pulses/m$^2$ | Average 8 pulses/m$^2$ |
| Resolution/Density (Submerged) | Average 2 pulses/m$^2$ | n/a |
| Nominal Pulse Spacing | 0.7 m | 0.35 m |
| Survey Altitude (AGL) | 400 m | 400 m |
| Survey speed | 60 knots | 60 knots |
| Field of View | 40º | 40º |
| Mirror Scan Rate | 80 lines per second | Uniform point spacing |
| Target Pulse Rate | 245 kHz | 245 kHz |
| Pulse Length | 1.5 ns | 3 ns |
| Laser Pulse Footprint Diameter | 28 cm | 8 cm |
| Central Wavelength | 532 nm | 1064 nm |
| Pulse Mode | Multiple Times Around (MTA) | Multiple Times Around (MTA) |
| Beam Divergence | 0.7 mrad | 0.2 mrad |
| Swath Width | 291 m | 291 m |
| Swath Overlap | 30 % | 30 % |
| Intensity | 16-bit | 16-bit |
| Accuracy | RMSE$_Z$ ≤ 18.5 cm | RMSE$_Z$ ≤ 18.5 cm |

To accurately solve for laser point position (geographic coordinates x, y and z), the positional coordinates of the airborne sensor and the attitude of the aircraft were recorded continuously throughout the lidar data collection mission. Position of the aircraft was measured twice per second (2 Hz) by an onboard differential GPS unit, and aircraft attitude was measured 200 times per second (200 Hz) as pitch, roll and yaw (heading) from an onboard inertial measurement unit (IMU). To allow for post-processing correction and calibration, aircraft and sensor position and attitude data are indexed by GPS time.



*Another photo taken by QSI's acquisition team shows an oblique aerial view of the mouth of the Klamath River at the Pacific Ocean, taken from the helicopter during lidar flights.*

# Digital Imagery

Aerial imagery was collected using an UltraCam XP and an UltraCam Falcon digital mapping camera (Table 6). The systems were gyro-stabilized and simultaneously collected panchromatic and multispectral (RGB, NIR) imagery.

**Table 6: Camera manufacturer's specifications**

| UltraCam XP/Falcon Specifications | |
|---:|:---|
| Focal Length | 100.5 mm |
| Data Format | RGB, NIR |
| RCD Pixel Size | 6.0 µm |
| Image Size | 17,310 x 11,310 pixels |
| Frame Rate | 2.0 sec (GPS triggered) |
| FOV | 55 x 37 deg |

For the Klamath River Topobathy project, 1,781 images were collected with 60% along track overlap and 40% sidelap between frames. The acquisition flight parameters were designed to yield a native pixel resolution of ≤ 15 cm. Orthophoto specifications particular to the Klamath River survey are shown in Table 7.

**Table 7: Project-specific orthophoto specifications**

| Digital Orthophotography Specifications | |
|---:|:---|
| Equipment | UltraCam XP/Falcon |
| Spectral Bands | Red, Green, Blue, NIR |
| Ground Sampling Distance | ≤ 15 cm |
| Along Track Overlap | ≥60% |
| Cross Track Overlap | ≥40% |
| Flight Altitude (AGL) | 2,500 meters |
| Data Format | 8-bit GeoTiff |

# Ground Survey

Ground control surveys, including base stations, aerial targets and ground survey points (GSPs), were conducted by QSI to support the airborne acquisition. Ground control data were used to geospatially correct the aircraft positional coordinate data and to perform quality assurance checks on final lidar data and orthoimagery products.



*QSI-Established Base*

## Base Stations

Base stations supported collection of ground survey points using real time kinematic (RTK), post processed kinematic (PPK), and fast static (FS) survey techniques. Base station locations were selected with consideration for satellite visibility, field crew safety, and optimal location for GSP coverage. QSI utilized four NGS monuments, two Leica SmartNet Real Time Network (RTN) base stations, two Oregon Real-time GNSS Network (ORGN) RTN base stations, and four newly-established monuments for the Klamath River lidar project (Table 8, Figure 4). New base stations were set using 5/8" x 30" rebar topped with stamped 2 ½ " aluminum caps. QSI's professional land surveyor, Evon P. Silvia (ORPLS#81104, CAPLS#9401) oversaw and certified the establishment of all base stations.

**Table 8: Base Stations utilized for the Klamath River acquisition. Coordinates are on the NAD83 (2011) datum, epoch 2010.00**

| Base Station ID | Latitude | Longitude | Ellipsoid (meters) | Base Station Type |
|---|---|---|---|---|
| AF8313 | 41° 49' 30.52025" | -122° 58' 24.29385" | 473.696 | NGS Monument |
| AF8314 | 41° 51' 50.48136" | -122° 43' 43.47429" | 544.379 | NGS Monument |
| DH6358 | 41° 21' 03.63961" | -123° 30' 09.86520" | 186.278 | NGS Monument |
| DH6353 | 41° 14' 25.69661" | -123° 39' 20.34297" | 99.125 | NGS Monument |
| KLAM_RTK_01 | 41° 55' 53.60915" | -122° 26' 30.05496" | 644.842 | QSI Monument |
| KLAM_RTK_02 | 41° 39' 41.28374" | -123° 26' 59.92257" | 254.391 | QSI Monument |
| KLAM_RTK_03 | 41° 16' 43.30246" | -123° 49' 58.88685" | 75.561 | QSI Monument |
| KLAM_RTK_04 | 41° 30' 34.28502" | -123° 59' 24.17923" | -15.150 | QSI Monument |
| ORKF | 42° 08' 36.16180" | -121° 48' 31.06952" | 1235.036 | Leica SmartNet RTN |
| P380 | 42° 15' 34.79886" | -121° 46' 46.85526" | 1391.280 | ORGN RTN |
| P784 | 41° 49' 50.92289" | -122° 25' 13.58557" | 802.702 | ORGN RTN |
| P154 | 41° 48' 25.48411" | -123° 21' 36.12405" | 320.323 | Leica SmartNet RTN |

To correct the continuously recorded onboard measurements of the aircraft position, QSI concurrently conducted multiple static Global Navigation Satellite System (GNSS) ground surveys (1 Hz recording frequency) over each base station. During post-processing, the static GPS data were triangulated with nearby Continuously Operating Reference Stations (CORS) using the Online Positioning User Service

(OPUS[1]) for precise positioning.  Multiple independent sessions over the same base station were processed to confirm antenna height measurements and to refine position accuracy.

## Ground Survey Points (GSPs)

Ground survey points were collected using RTK, PPK, and FS survey techniques. For an RTK survey, a roving receiver receives corrections from a nearby base station or Real-Time Network (RTN) via radio or cellular network, enabling rapid collection of points with relative errors less than 1.5 cm horizontal and 2.0 cm vertical. PPK and FS surveys compute these corrections during post-processing to achieve comparable accuracy. RTK and PPK surveys record data while stationary for at least five seconds, calculating the position using at least three one-second epochs. FS surveys record observations for up to fifteen minutes on each GSP in order to support longer baselines for post-processing. All GSP measurements were made during periods with a Position Dilution of Precision (PDOP) of ≤ 3.0 with at least six satellites in view of the stationary and roving receivers. See Table 9 for QSI ground survey equipment specifications.

GSPs were collected in areas where good satellite visibility was achieved on paved roads and other hard surfaces such as gravel or packed dirt roads. GSP measurements were not taken on highly reflective surfaces such as center line stripes or lane markings on roads due to the increased noise seen in the laser returns over these surfaces. GSPs were collected within as many flightlines as possible; however, the distribution of GSPs depended on ground access constraints and base station locations and may not be equitably distributed throughout the study area (Figure 4).

**Table 9: Trimble equipment identification**

| Receiver Model | Antenna | OPUS Antenna ID | Use |
| --- | --- | --- | --- |
| Trimble R7 GNSS | Zephyr GNSS Geodetic Model 2 RoHS | TRM57971.00 | Static |
| Trimble R8 | Integrated Antenna R8 Model 2 | TRM_R8_GNSS | Rover |

---

[1] OPUS is a free service provided by the National Geodetic Survey to process corrected base station positions. http://www.ngs.noaa.gov/OPUS/.

## Aerial Targets

Aerial targets were identified throughout the project area prior to imagery acquisition in order to geo-spatially correct the orthoimagery (Figure 4).  Air targets used for the Klamath River project consisted of spray-painted chevrons and existing permanent photo-identifiable features painted on asphalt such as handicap parking signs, stop bars, and turn lane arrows. Each target was precisely located using one FS point.



## Land Cover Class

In addition to ground survey points, land cover class check points were collected throughout the study area to evaluate vertical accuracy. Vertical accuracy statistics were calculated for all land cover types to assess confidence in the lidar derived ground models across land cover classes (Table 10, see Lidar Accuracy Assessments).

**Table 10: Land Cover Types and Descriptions**

| Land cover type | Land cover code | Example | Description | Accuracy Assessment Type |
|---|---|---|---|---|
| Shrubland | SHRUB |  | Maintained or low growth herbaceous grasslands | VVA |
| Tall Grass | TALL_GRASS |  | Herbaceous grasslands in advanced stages of growth | VVA |
| Bare Earth | BARE, BE |  | Areas of bare earth surface | NVA |
| Urban | URBAN |  | Areas dominated by urban development, including parks | NVA |

**Figure 4: Ground survey location map**

**Legend:**
- Base Station
- Vegetated Check Point
- Non-Vegetated Check Point
- Air Target Point
- Ground Control Point
- Wetted Edge Check Point
- Bathymetric Check Point
- Klamath River Site Boundary (72,030 acres)
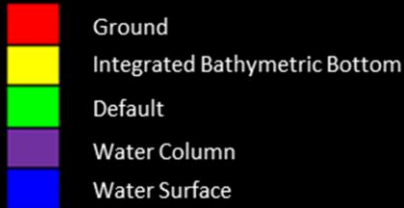
This 2.0 meter cross section shows a view of Iron Gate Reservoir in the Klamath Reservoirs AOI, extending to a maximum depth of 40 meters. Displayed points are from the integrated topobathymetric dataset colored by laser point classification.

Legend:
- Ground
- Integrated Bathymetric Bottom
- Default
- Water Column
- Water Surface
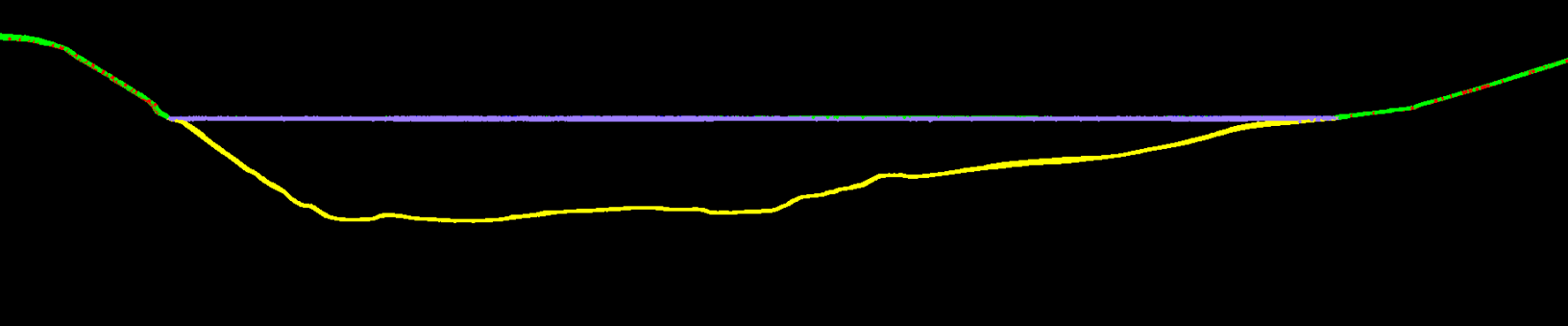
## Topobathymetric Lidar Data and Sonar Integration

Upon completion of data acquisition, QSI processing staff initiated a suite of automated and manual techniques to process the data into the requested deliverables. Processing tasks included GPS control computations, smoothed best estimate trajectory (SBET) calculations, kinematic corrections, calculation of laser point position, sensor and data calibration for optimal relative and absolute accuracy, and lidar point classification (Table 11).

Riegl's RiProcess software was used to facilitate bathymetric return processing. Once bathymetric points were differentiated, they were spatially corrected for refraction through the water column based on the angle of incidence of the laser. QSI refracted water column points using QSI's proprietary LAS processing software, Las Monkey.  The resulting point cloud data were classified using both manual and automated techniques.

GMA performed all multibeam and sweep sonar data acquisitions and used Caris HIPS v. 10 to process and edit raw track lines to remove any noise and to evaluate the data for visual anomalies. Sonar data was provided to QSI in LAS 1.4 format. QSI imported the multibeam and sweep sonar, as Class 40 (Bathymetric Bottom), into the existing topobathymetric lidar dataset using Bentley Microstation and Terrasolid software. Processing methodologies were tailored for the landscape. Brief descriptions of these tasks are shown in Table 12.

**Table 11: ASPRS LAS classification standards applied to the Klamath River dataset**

| Classification Number | Classification Name | Classification Description |
|---|---|---|
| 1 | Default/Unclassified | Laser returns that are not included in the ground class, composed of vegetation and anthropogenic features |
| 1-O | Default/Unclassified Overlap | Flightline edge clip that is withheld because it does not contribute to the utility of the dataset, but may be maintained as a reference |
| 2 | Ground | Laser returns that are determined to be ground using automated and manual cleaning algorithms |
| 3 | Low Vegetation | Laser returns between 0.25 and 2 meters that were classified as vegetation using an automated routine |
| 4 | Medium Vegetation | Laser returns between 2 and 5 meters that were classified as vegetation using an automated routine |
| 5 | High Vegetation | Laser returns above 5 meters that were classified as vegetation using an automated routine |
| 7 | Noise | Laser returns that are often associated with birds, scattering from reflective surfaces, or artificial points below the ground surface |
| 9 | NIR Water Surface | NIR laser returns that are determined to be water using automated and manual cleaning algorithms |
| 17 | Bridge | Bridge decks |
| 20 | Ignored Ground | Ground points proximate to water's edge breaklines; ignored for correct model creation |
| 40 | Lidar Bathymetric Bottom | Refracted Riegl sensor returns that fall within the water's edge breakline which characterize the submerged topography and integrated sonar data |
| 41 | Green Water Surface | Green laser returns that are determined to be water surface points using automated and manual cleaning algorithms |
| 45 | Water Column | Refracted Riegl sensor returns that are determined to be water using automated and manual cleaning algorithms |
| 80 | Sonar Bathymetric Bottom | Binned sonar returns that were collected with a multi-transducer sonar sweep system |
| 81 | Sonar Bathymetric Bottom | Binned sonar returns that were collected with a multibeam sonar system |

**Table 12: Lidar and sonar integration processing workflow**

| Lidar Processing Step | Software Used | Processor |
|---|---|---|
| Resolve kinematic corrections for aircraft position data using kinematic aircraft GPS and static ground GPS data. Develop a smoothed best estimate of trajectory (SBET) file that blends post-processed aircraft position with sensor head position and attitude recorded throughout the survey. | POSPac MMS v.8.2 | QSI |
| Calculate laser point position by associating SBET position to each laser point return time, scan angle, intensity, etc. Create raw laser point cloud data for the entire survey in *.las (ASPRS v. 1.4) format. Convert data to orthometric elevations by applying a geoid correction. | RiProcess v1.8.5 TerraMatch v.18 | QSI |
| Import raw laser points into manageable blocks (less than 500 MB) to perform manual relative accuracy calibration and filter erroneous points. Classify ground points for individual flight lines. | TerraScan v.18 | QSI |
| Using ground classified points per each flight line, test the relative accuracy. Perform automated line-to-line calibrations for system attitude parameters (pitch, roll, heading), mirror flex (scale) and GPS/IMU drift. Calculate calibrations on ground classified points from paired flight lines and apply results to all points in a flight line. Use every flight line for relative accuracy calibration. | TerraMatch v.18 RiProcess v.1.8.2 | QSI |
| Apply refraction correction to all subsurface returns. | Las Monkey 2.3 (QSI proprietary software) | QSI |
| *Collect multibeam and sweep sonar. Process and edit raw track lines to remove any noise. Evaluate data for visual anomalies and perform quality assurance checks. | Caris HIPS v. 10 | GMA |
| Import multibeam Sonar data into LiDAR point cloud | TerraScan v.18 TerraModeler v.18 | QSI |
| Classify resulting data to ground and other client designated ASPRS classifications (Table 11). Assess statistical absolute accuracy via direct comparisons of ground classified points to ground control survey data. | TerraScan v.18 TerraModeler v.18 | QSI |
| Generate bare earth models as triangulated surfaces. Generate highest hit models as a surface expression of all classified points. Export all surface models in ERDAS Imagine (.img) format 1 meter pixel resolution. | Las Product Creator 3.0 (QSI proprietary software) | QSI |
| Export intensity images as GeoTIFFs at a 0.5 meter pixel resolution. | Las Product Creator 3.0 (QSI proprietary software) | QSI |

*See Appendix B for detailed explanation of sonar processing*

# Bathymetric Refraction

Green lidar pulses that enter the water column must have their position corrected for refraction of the light beam as it passes through the water and its resulting decreased speed. QSI has developed proprietary software (Las Monkey) to perform this processing based on Snell's law. The first step is to develop a water surface model (WSM) from the NIR lidar water surface returns.

Depending on the degree of water level fluctuation due to temporal changes in water elevation, QSI implemented two different methods to generate WSMs. For water bodies considered "calm" with relatively static water levels, the WSM used for refraction is generated using NIR points within the breaklines defining the water's edge. Points are filtered and edited to obtain the most accurate representation of the water surface and are used to create a water surface model TIN.

For water bodies exposed to tidal or wave action, the method of WSM generation factors in significant temporal changes in water surface elevation over the time of acquisition. NIR lidar returns are used to determine the water surface level and water surface points are classified for both forward and reverse look directions of the green scanner. The points are filtered and edited to obtain the most accurate representation of the water surface and are used to generate a WSM for each flight line and look direction. Each look direction (forward and reverse) are modeled separately to correctly model short duration time dependent surface changes (e.g. waves) that change between the times that each look direction records a unique location. The WSM created is raster based with an associated surface normal vector to obtain the most accurate angle of incidence during refraction.

Once all WSMs are generated, the Las Monkey refraction software then intersects the partially submerged green pulses with the WSM to determine the angle of incidence with the water surface and the submerged component of the pulse vector. This provides the information necessary to correct the position of underwater points by adjusting the submerged vector length and orientation. After refraction, the points are compared against bathymetric check points to assess accuracy.

Both methods of WSM generation were implemented for the Klamath River AOI project. At the Klamath River mouth, where the river empties into the Pacific Ocean, the method incorporating tidal and wave action was used to generate the WSM. All other areas of the Klamath River AOI were refracted using a WSM that assumed water levels remained relatively static during acquisition.

# Topobathymetric DEMs

Bathymetric bottom lidar returns can be limited by depth, water clarity, and bottom surface reflectivity. Water clarity and turbidity affect the depth penetration capability of the green wavelength lidar with returning laser energy diminishing by scattering throughout the water column. Additionally, the bottom surface must be reflective enough to return remaining laser energy back to the sensor at a detectable level. Likewise, the multibeam and sweep sonar collection is limited by obstructions within the river channel and proximity to the shoreline, due to safety procedures for crew and equipment. Therefore, it is not unexpected to have no bathymetric bottom returns in turbid, non-reflective, or obstructed areas.

As a result, creating digital elevation models (DEMs) presents a challenge with respect to interpolation of areas with no returns. Traditional DEMs are "unclipped", meaning areas lacking ground returns are interpolated from neighboring ground returns (or breaklines in the case of hydro-flattening), with the assumption that the interpolation is close to reality. In bathymetric modeling, these assumptions are prone to error because a lack of bathymetric returns can indicate a change in elevation that the sensors can no longer map due to increased or decreased depths. The resulting void areas may suggest varying depths, rather than similar elevations from neighboring bathymetric bottom returns. Therefore, QSI created a final water polygon with bathymetric coverage to delineate areas with successfully mapped bathymetry from lidar and sonar integration. This shapefile was used to clip the extent of the final integrated topobathymetric model to avoid false triangulation (interpolation from TIN'ing) across areas in the water with no mapped bathymetry.
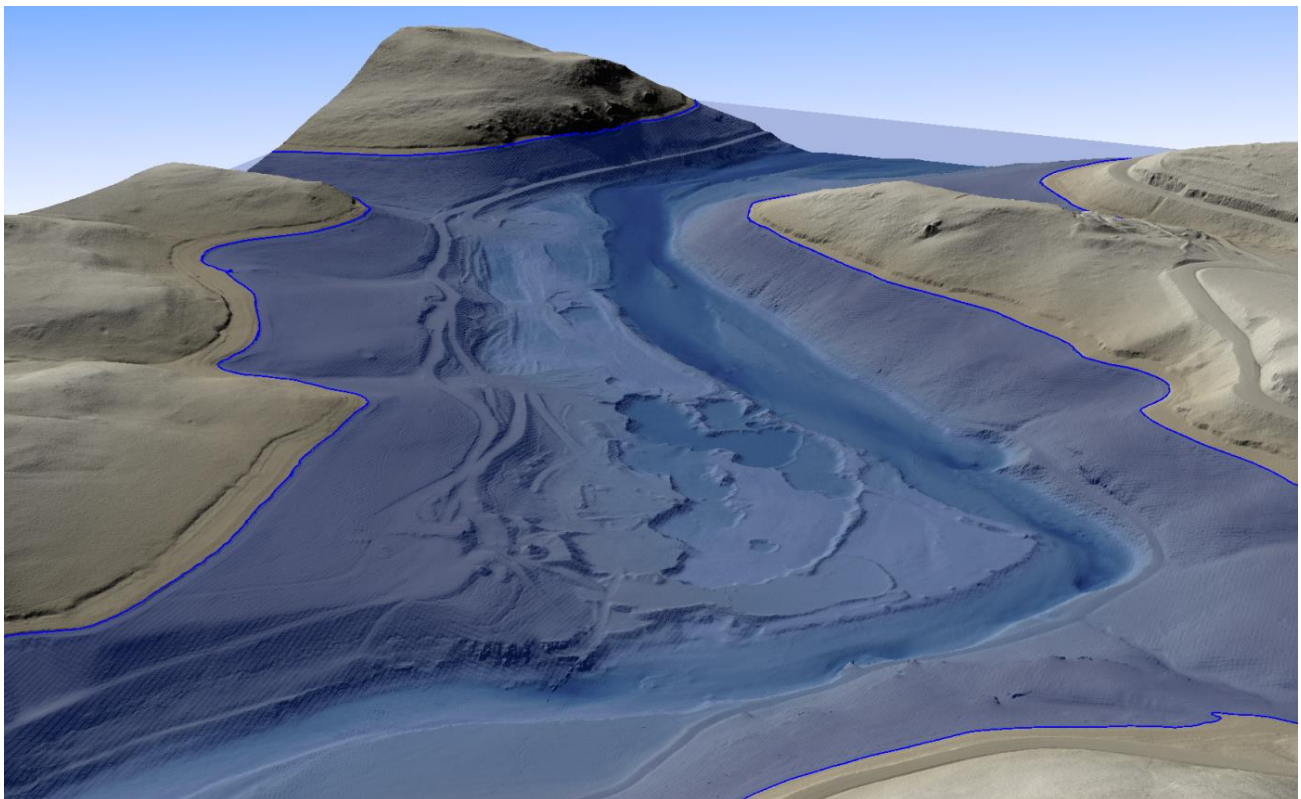


**Figure 5: A view looking down at the Iron Gate Reservoir showing bathymetric depths up to 38 meters. This image was created from the integrated topobathymetric bare earth model colored by elevation. A simulated water level is inserted into the image at an elevation of 707 meters.**

# Feature Extraction

## Hydroflattening and Water's Edge Breaklines

The Klamath River and other water bodies within the project area were flattened to a consistent water level. Bodies of water that were flattened include lakes and other closed water bodies with a surface area greater than 2 acres, all streams and rivers that are nominally wider than 30 meters, all tidal waters bordering the project, and select smaller bodies of water as feasible. The hydroflattening process eliminates artifacts in the digital terrain model caused by both increased variability in ranges or dropouts in laser returns due to the low reflectivity of water.

Hydroflattening of closed water bodies was performed through a combination of automated and manual detection and adjustment techniques designed to identify water boundaries and water levels. Boundary polygons were developed using an algorithm which weights lidar-derived slopes, intensities, and return densities to detect the water's edge. The water edges were then manually reviewed and edited as necessary.

Once polygons were developed the initial ground classified points falling within water polygons were reclassified as water points to omit them from the final ground model.  Elevations were then obtained from the filtered lidar returns to create the final breaklines. Lakes were assigned a consistent elevation for an entire polygon while rivers were assigned consistent elevations on opposing banks and smoothed to ensure downstream flow through the entire river channel.

Water boundary breaklines were then incorporated into the hydroflattened DEM by enforcing triangle edges (adjacent to the breakline) to the elevation values of the breakline.  This implementation corrected interpolation along the hard edge.

# Contours

Contour generation from lidar point data required a thinning operation in order to reduce contour sinuosity. The thinning operation reduced point density where topographic change is minimal (i.e., flat surfaces) while preserving resolution where topographic change was present. Model key points were selected from the ground classified points with the spacing decreased in regions with high surface curvature. Generation of model key points eliminated redundant detail in terrain representation, particularly in areas of low relief, and provided for a more manageable dataset. Contours were produced through TerraModeler by interpolating between the model key points at even elevation increments.

Elevation contour lines were then intersected with ground point density raster models and a confidence field was added to each contour line. Contours which crossed areas of high point density have high confidence levels, while contours which crossed areas of low point density have low confidence levels. Areas with low ground point density are commonly beneath buildings and bridges, in locations with dense vegetation, over water, and in other areas where laser penetration to the ground surface was impeded (Figure 6).
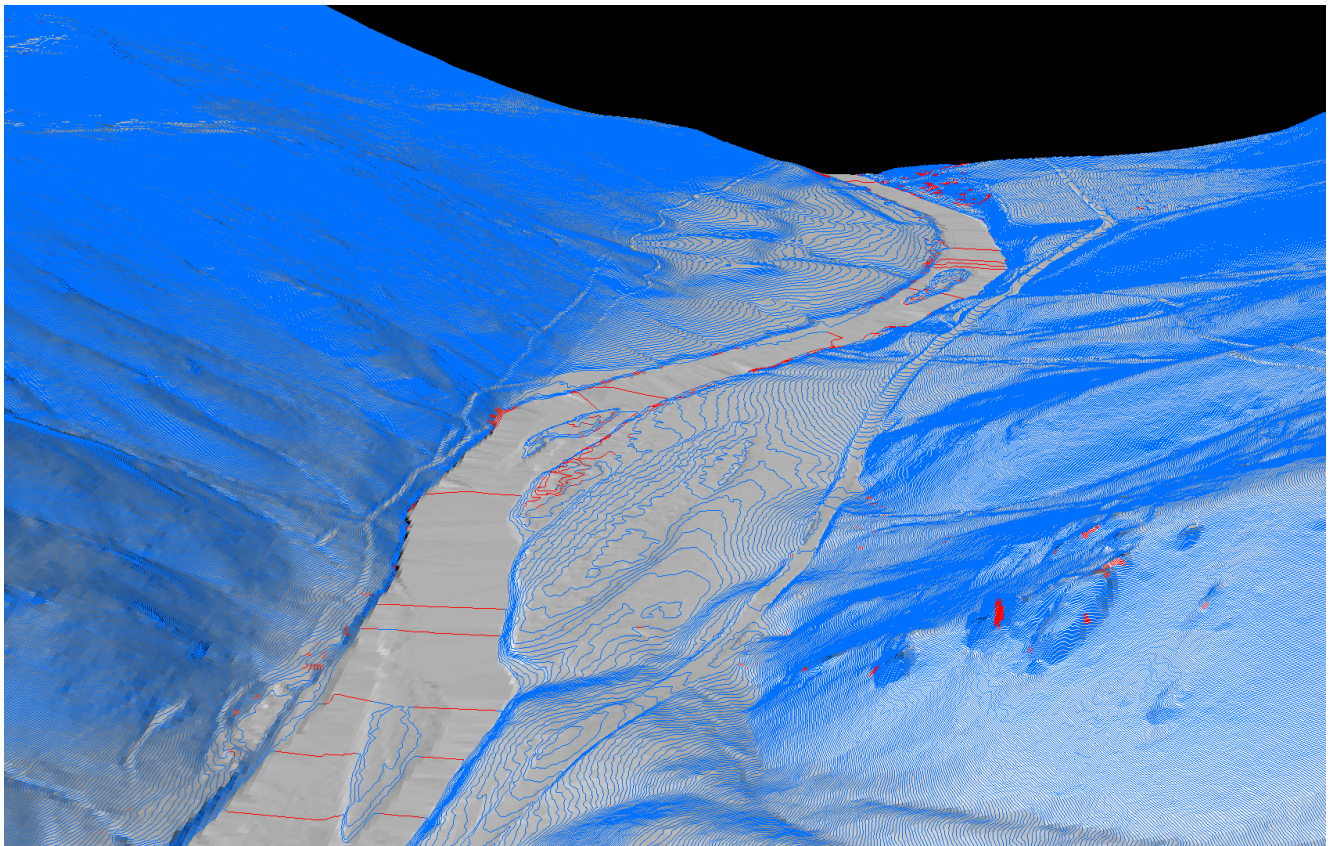


**Figure 6: Contours draped over the Klamath River bare earth elevation model located east of Copco Lake. Blue contours represent high confidence while the red contours represent low confidence.**

# Digital Imagery

The collected digital photographs went through multiple processing steps to create final orthophoto products. Initially, images were corrected for geometric distortion to yield level02 image files.  Next, images were color balanced and levels were adjusted to exploit the full 14-bit histogram and finally output as level03 pan-sharpened 8bit TIFF images.  Camera position and orientation were calculated by linking the time of image capture to the smoothed best estimate of trajectory (SBET).  Within Inpho's Match AT softcopy photogrammetric software, analytical aerial triangulation was performed using ground control, automatically generated tie points, and camera calibration information.

Adjusted images were orthorectified using the lidar-derived ground model to remove displacement effects from topographic relief inherent in the imagery. The resulting orthos were mosaicked within Inpho's OrthoVista blending seams and applying automated project color-balancing.  The final mosaics were inspected and edited for seam cutlines across above ground features such as buildings and other man-made features.  Special care was taken to eliminate glare on the water surface, in some instances this resulted in introducing tree lean along the river shoreline. The processing workflow for orthophotos is summarized in Table 13.

**Table 13: Orthophoto processing workflow**

| Orthophoto Processing Step | Software Used |
|---|---|
| Resolve GPS kinematic corrections for the aircraft position data using kinematic aircraft GPS (collected at 2 Hz) and static ground control data. | Inertial Explorer v8.7 |
| Develop a smooth best estimate trajectory (SBET) file that blends post-processed aircraft position with attitude data. Sensor heading, position, and attitude are calculated throughout the survey. | Inertial Explorer v8.7 |
| Create an exterior orientation file (EO) for each photo image with omega, phi, and kappa. | Inertial Explorer v8.7 |
| Convert Level 00 raw imagery data into geometrically corrected Level 02 image files. | UltraMap v4 |
| Apply radiometric adjustments to Level 02 image files to create Level 03 Pan-sharpened TIFFs. | UltraMap v4 |
| Apply EO to photos, measure ground control points and perform aerial triangulation. | Inpho Match AT v8 |
| Use lidar derived DEM to create distortion free ortho images. | Inpho OrthoMaster v8 |
| Mosaic orthorectified imagery, blending seams between individual photos and correcting for radiometric differences between photos. | Inpho OrthoVista/SeamEditor v8 |

This 1.0 meter cross section shows a view of the Klamath River project area colored by laser return echo.

Legend: Only Echo (green), First of Many (red), Intermediate (yellow), Last of Many (cyan)
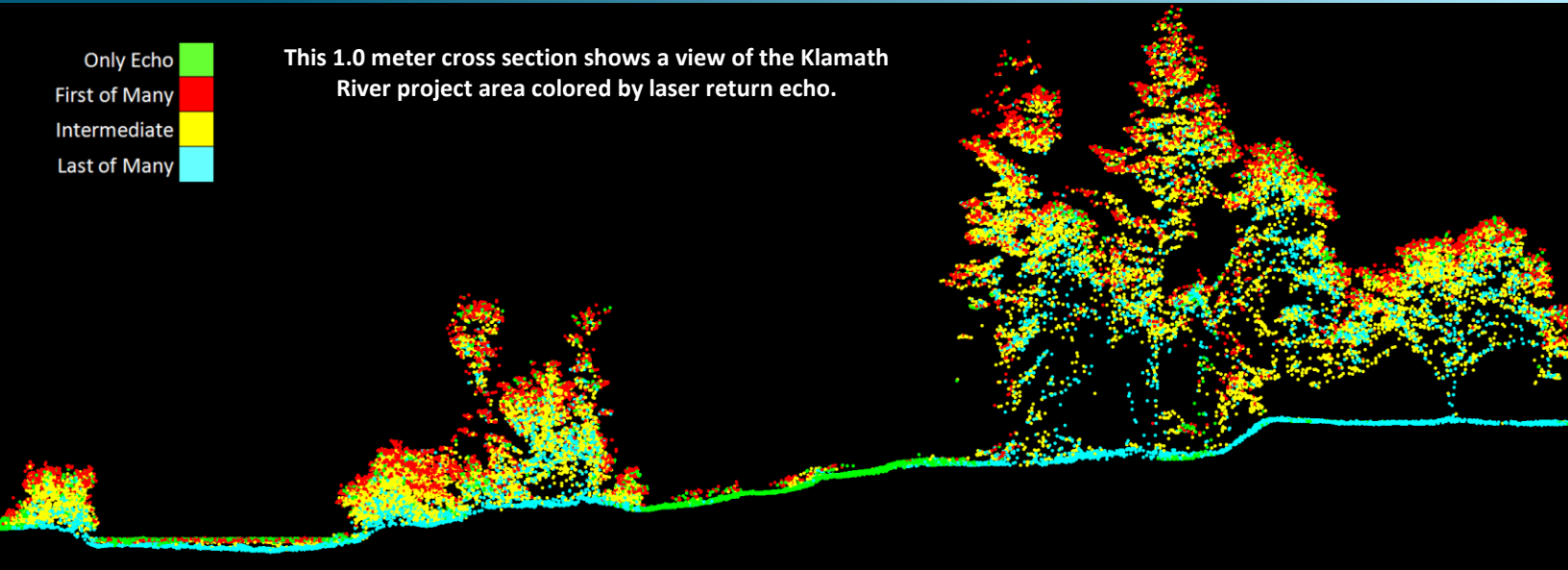
## Bathymetric Lidar

An underlying principle for collecting hydrographic lidar data is to survey near-shore areas that can be difficult to collect with other methods, such as sonar. Lidar excels in shallow bathymetric environments, particularly over large areas, but bathymetric detection at greater depths is limited up to the laser depth penetration range. Deep bathymetric environments are more favorable to sonar collection methods due to the sound wave's greater capacity to propagate through water. Sonar data may be used to compliment topobathymetric lidar surveys by providing bathymetric depth measurements in areas exceeding the laser penetration range. Sites like the Klamath River AOI that exhibit shallow and deep bathymetric environments offer an opportunity to integrate sonar with lidar data to create a comprehensive seamless topobathymetric model of the project site.

All available multibeam and sweep sonar data was integrated with the final topobathymetric lidar dataset. In order to assess the overall integrated bathymetric dataset, several parameters were considered; depth penetrations below the water surface, bathymetric return density, and spatial accuracy.

## Mapped Bathymetry and Integrated Coverage

QSI reviewed bathymetric coverage and void results for the Klamath River project in lidar-only areas, as well as the fully integrated lidar and sonar dataset. Insufficiently mapped areas were identified by triangulating bathymetric bottom points with an edge length maximum of 4.56 meters. This ensured all areas of no returns (> 9 $m^2$), were identified as data voids.

In total, approximately 65.65% of the Klamath River and Reservoirs sites were mapped with bathymetric bottom data. Additionally, bathymetric coverage increased from 4,686 acres with lidar only data, to 6,466 acres after sonar integration.

QSI also reviewed the mapped depths of identified coverage areas; in lidar-only areas, 47.37% of bathymetric bottom returns were up to one foot deep. In fully integrated areas, depths of up to 47 meters were mapped. Table 15 and Table 16 below provide depth and coverage information for the lidar-only sites, as well as the full, integrated dataset.

**Table 14: Fully integrated lidar and sonar bathymetric bottom coverage results by depth**

| Depth (m) | Percent of "Covered" Area (%) | Total Area (acres) |
|---|---|---|
| < 5 | 33.50% | 659.73 |
| 5 - 10 | 18.85% | 371.30 |
| 10 -15 | 14.83% | 292.00 |
| 15 - 20 | 12.61% | 248.39 |
| 20 -25 | 8.49% | 167.16 |
| 25 - 30 | 4.12% | 81.22 |
| 30 - 35 | 3.85% | 75.73 |
| 35 - 40 | 2.87% | 56.55 |
| 40 - 45 | 0.86% | 16.86 |
| 45 - 47 | 0.02% | 0.47 |

**Table 15: Lidar-only bathymetric bottom coverage results by depth**

| Depth (m) | Percent of "Covered" Area (%) | Area (acres) |
|---|---|---|
| < 0.49 | 23.57% | 1,029.97 |
| 0.49 - 1.0 | 23.80% | 1,039.74 |
| 1.0 - 1.49 | 18.82% | 822.35 |
| 1.5 - 1.99 | 13.55% | 591.97 |
| 2.0 - 2.49 | 9.08% | 396.82 |
| 2.5 - 2.99 | 6.12% | 267.61 |
| 3.0 - 3.49 | 3.60% | 157.09 |
| 3.5 - 3.99 | 1.28% | 56.15 |
| 4.0 - 4.49 | 0.17% | 7.25 |
| 4.5 - 4.99 | 0.01% | 0.34 |
| > 5.0 | 0.00% | 0.04 |
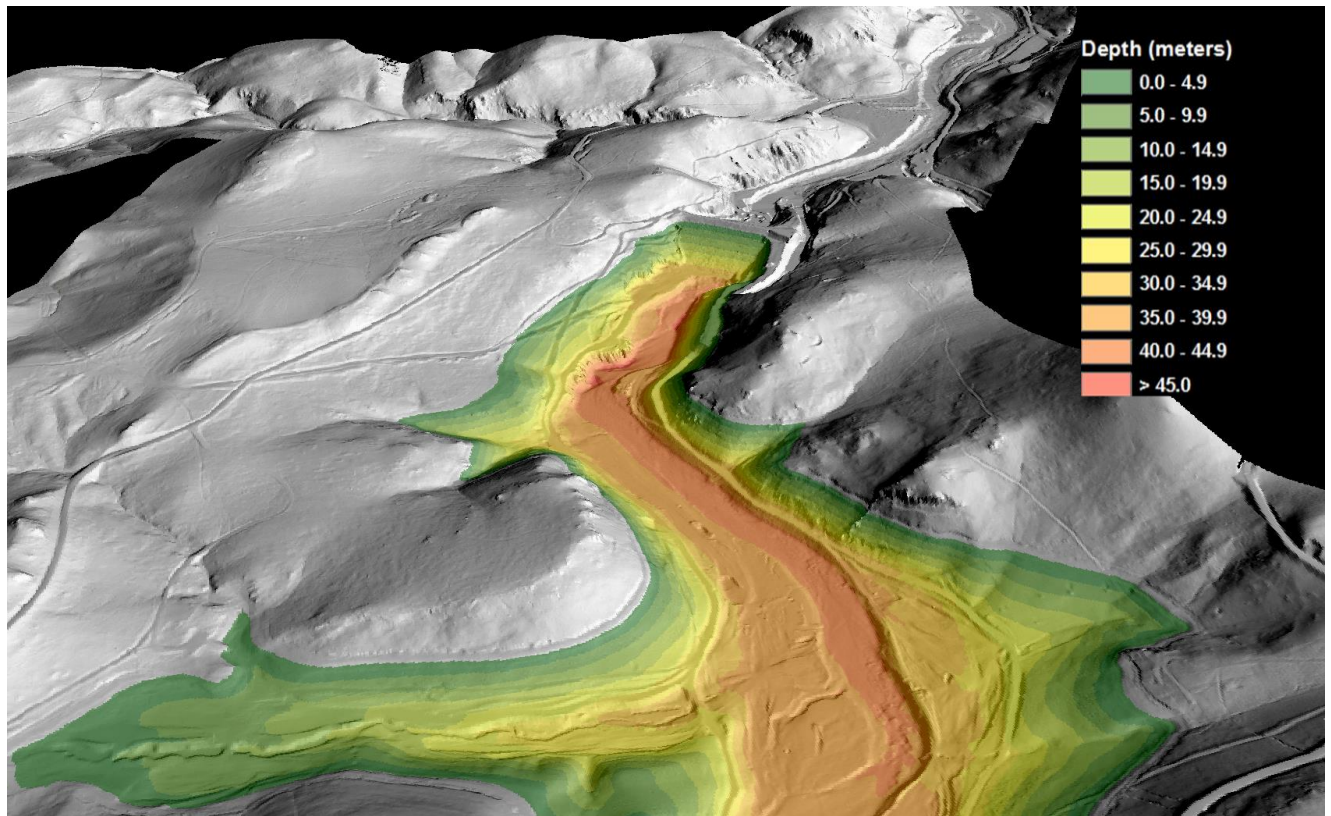
**Figure 7: A south facing view looking down at the Iron Gate Reservoir showing bathymetric depths up to 47 meters. This image was created from the integrated topobathymetric bare earth hill shade overlain by a water depth model colored by depth.**

# Lidar Point Density

## First Return Point Density

The acquisition parameters were designed to acquire a minimum first-return density of $\geq 8$ points/m$^2$. Due to the low AGL and slower flight speed of the helicopter used to acquire lidar data, point density results were anticipated to be much higher than contract requirements.

First return density describes the density of pulses emitted from the laser that return at least one echo to the system. Multiple returns from a single pulse were not considered in first return density analysis. Some types of surfaces (e.g., breaks in terrain, water and steep slopes) may have returned fewer pulses than originally emitted by the laser. First returns typically reflect off the highest feature on the landscape within the footprint of the pulse. In forested or urban areas the highest feature could be a tree, building or power line, while in areas of unobstructed ground, the first return will be the only echo and represents the bare earth surface.

The average first-return density of the Klamath River lidar project was 49.20 points/m$^2$ (Table 16). The statistical and spatial distributions of all first return densities per 100 m x 100 m cell are portrayed in Figure 8 and Figure 10.

## Bathymetric and Ground Classified Point Densities

The density of ground classified lidar and bathymetric bottom returns were also analyzed for this project. Terrain character, land cover, and ground surface reflectivity all influenced the density of ground surface returns. In vegetated areas, fewer pulses may have penetrated the canopy, resulting in lower ground density. Similarly, the density of bathymetric bottom returns was influenced by turbidity, depth, and bottom surface reflectivity. In turbid areas, fewer pulses may have penetrated the water surface, resulting in lower bathymetric density.

The ground and bathymetric bottom classified density of lidar data for the Klamath River project was 5.37 points/m$^2$ (Table 16). The statistical and spatial distributions ground classified and bathymetric bottom return densities per 100 m x 100 m cell are portrayed in Figure 9 and Figure 11.

Additionally, acquisition parameters for the Klamath River project specified an average bathymetric bottom return density value of $\geq 2$ points/m$^2$. Bathymetric bottom returns were calculated for areas containing at least one bathymetric bottom return. Areas lacking bathymetric returns were not considered in calculating an average density value. Within the successfully mapped area, a bathymetric bottom return density of 9.18 points/m$^2$ was achieved.

**Table 16: Average lidar point densities**

| Density Type | Point Density |
|---|---|
| First Returns | 49.20 points/m² |
| Ground and Bathymetric Bottom Classified Returns | 5.37 points/m$^2$ |
| Bathymetric Bottom Classified Returns | 9.18 points/m² |
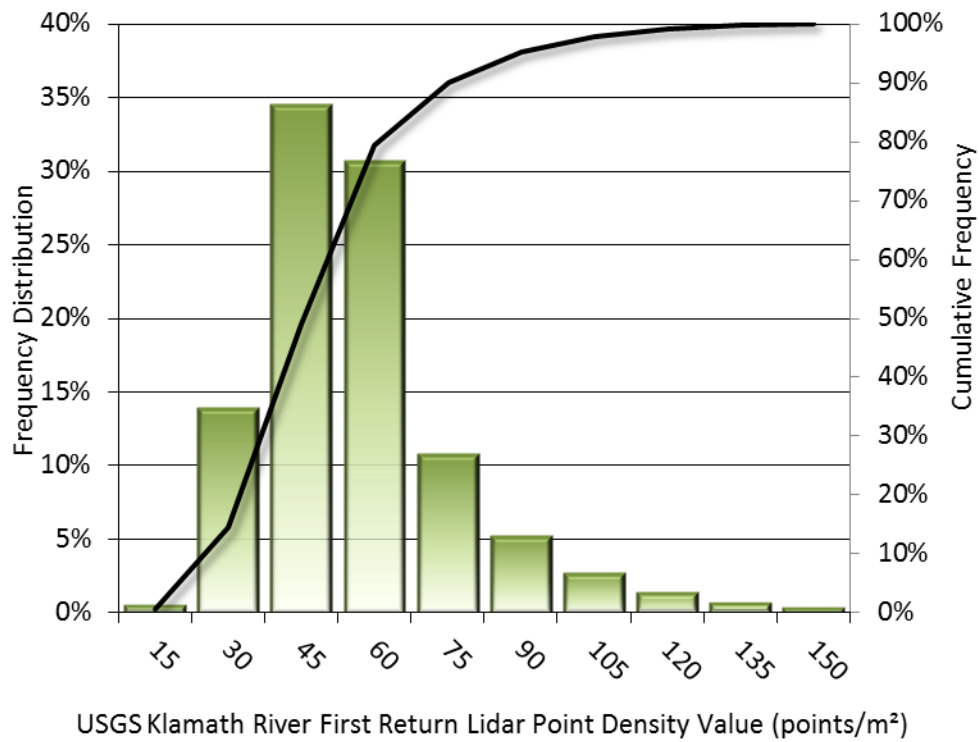
**Figure 8: Frequency distribution of first return densities per 100 x 100 m cell**
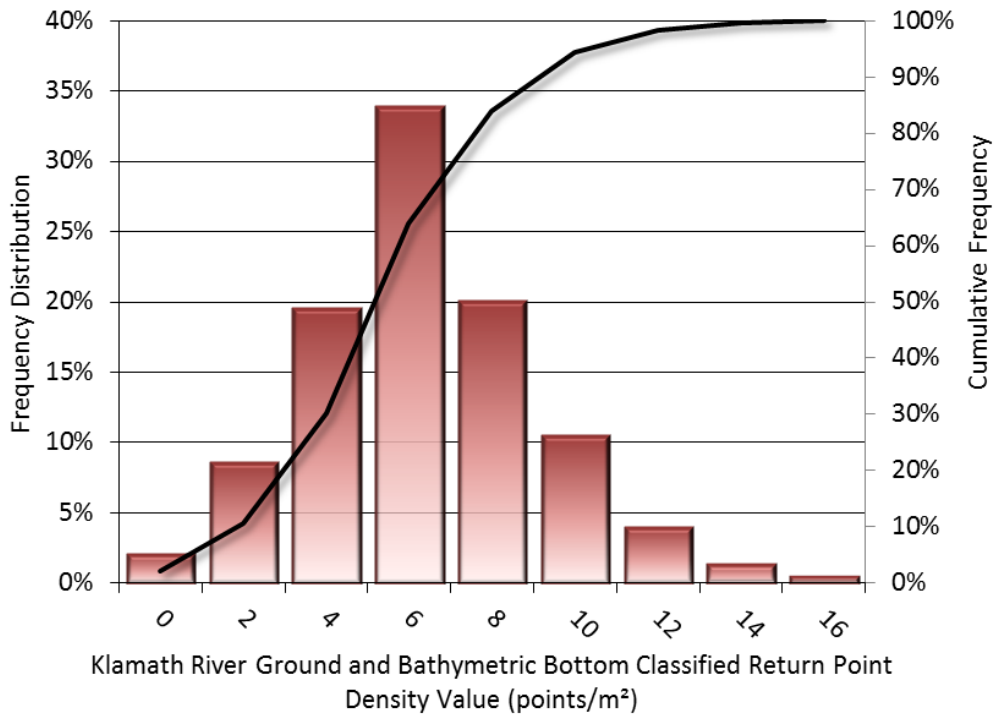


**Figure 9: Frequency distribution of ground and bathymetric bottom classified return densities per 100 x 100 m cell**

**Klamath River First Return Lidar Point Density**

points/meter$^2$

- 2.8 - 7.9
- 8.0 - 14.9
- 15.0 - 29.9
- 30.0 - 44.9
- 45.0 - 59.9
- 60.0 - 74.9
- 75.0 - 90.0
- 90.1 - 248.5
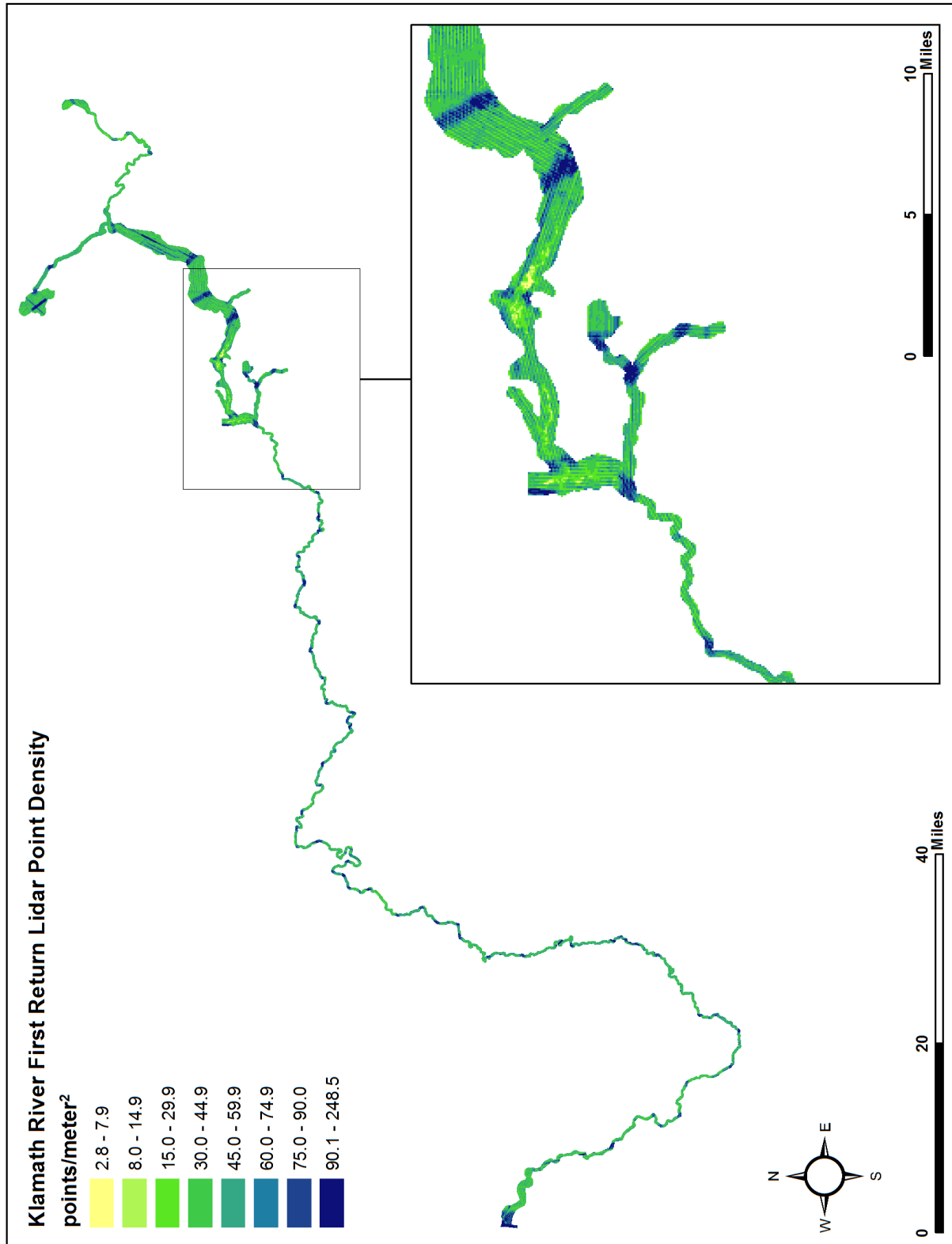
**Figure 10: First return Lidar point density map for the Klamath River site (100 m x 100 m cells)**
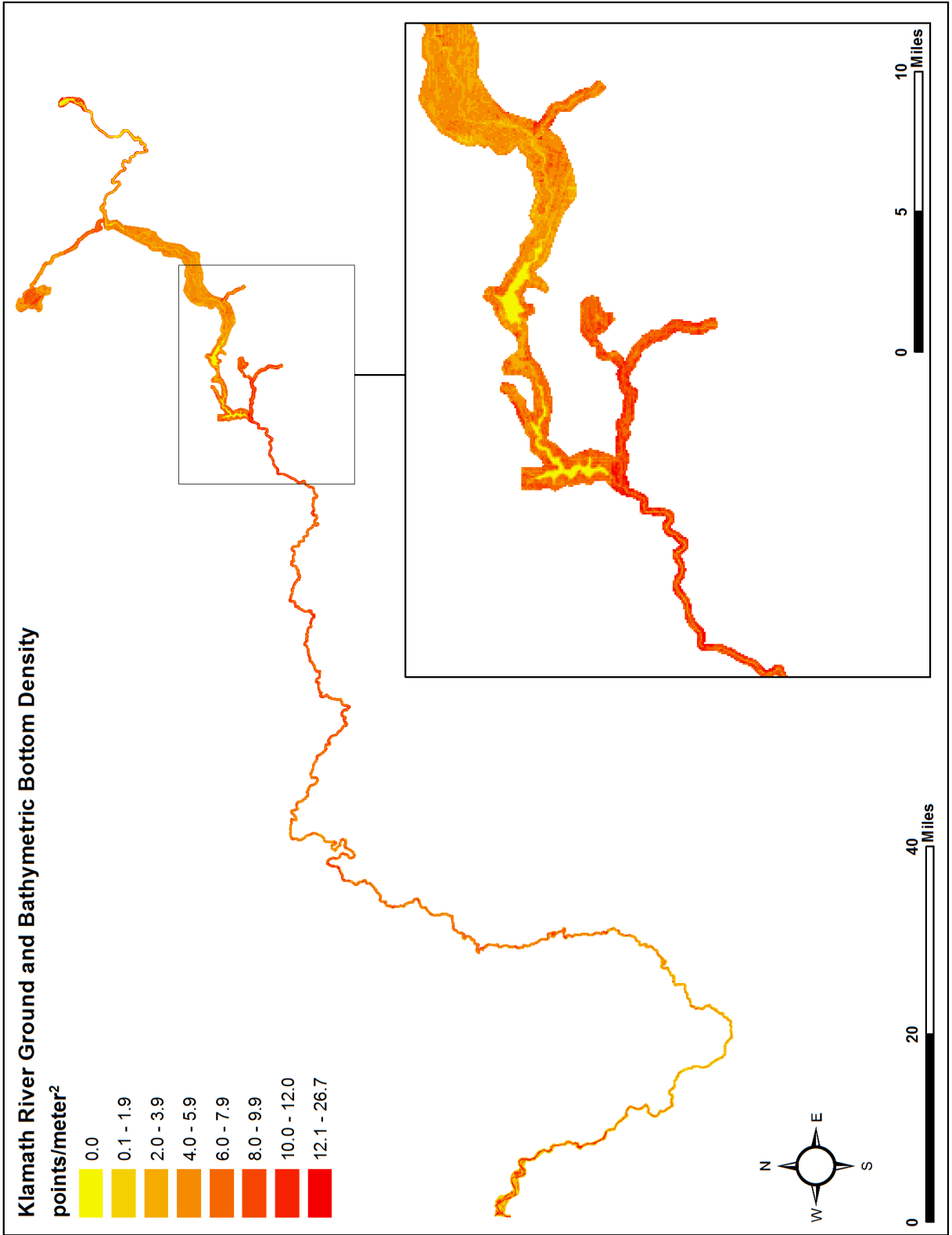
**Figure 11: LiDAR-derived Ground and bathymetric bottom density map for the Klamath River site (100 m x 100 m cells)**

# Lidar Accuracy Assessments

The accuracy of the lidar data collection can be described in terms of absolute accuracy (the consistency of the data with external data sources) and relative accuracy (the consistency of the dataset with itself). See Appendix A for further information on sources of error and operational measures used to improve relative accuracy.

## Lidar Non-Vegetated Vertical Accuracy

Absolute accuracy was assessed using Non-vegetated Vertical Accuracy (NVA) reporting designed to meet guidelines presented in the FGDC National Standard for Spatial Data Accuracy[2]. NVA compares known ground quality assurance point data collected on open, bare earth surfaces with level slope (<20°) to the triangulated surface generated by the unclassified lidar point cloud as well as the derived gridded bare earth DEM. NVA is a measure of the accuracy of lidar point data in open areas where the lidar system has a high probability of measuring the ground surface and is evaluated at the 95% confidence interval (1.96 * RMSE), as shown in Table 17.

The mean and standard deviation (sigma $\sigma$) of divergence of the ground surface model from ground check point coordinates are also considered during accuracy assessment. These statistics assume the error for x, y and z is normally distributed, and therefore the skew and kurtosis of distributions are also considered when evaluating error statistics. For the Klamath River survey, 21 ground check points were collected over non-vegetated surfaces, with resulting non-vegetated vertical accuracy of 0.074 meters, as compared to the unclassified LAS and 0.080 meters against the bare earth DEM, with 95% confidence (Figure 12 and Figure 13).

QSI also assessed absolute accuracy using 901 ground control points. Although these points were used in the calibration and post-processing of the lidar point cloud, they still provide a good indication of the overall accuracy of the lidar dataset, and therefore have been provided in Table 17 and Figure 14.

---

[2] Federal Geographic Data Committee, ASPRS POSITIONAL ACCURACY STANDARDS FOR DIGITAL GEOSPATIAL DATA EDITION 1, Version 1.0, NOVEMBER 2014. http://www.asprs.org/PAD-Division/ASPRS-POSITIONAL-ACCURACY-STANDARDS-FOR-DIGITAL-GEOSPATIAL-DATA.html.

**Table 17: Absolute accuracy (NVA) results**

| | NVA - Ground Check Points (LAS) | NVA - Ground Check Points (DEM) | Ground Control Points |
|---|---|---|---|
| **Absolute Vertical Accuracy** | | | |
| **Sample** | 21 points | 21 points | 901 points |
| **95% Confidence (1.96*RMSE)** | 0.074 m | 0.080 m | 0.059 m |
| **Average** | -0.002 m | -0.005 m | -0.015 m |
| **Median** | 0.001 m | -0.003 m | -0.015 m |
| **RMSE** | 0.038 m | 0.041 m | 0.030 m |
| **Standard Deviation (1σ)** | 0.039 m | 0.042 m | 0.026 m |



USGS Klamath River Non-Vegetated Vertical Accuracy (LAS)
LiDAR Surface Deviation from Control Survey (m)
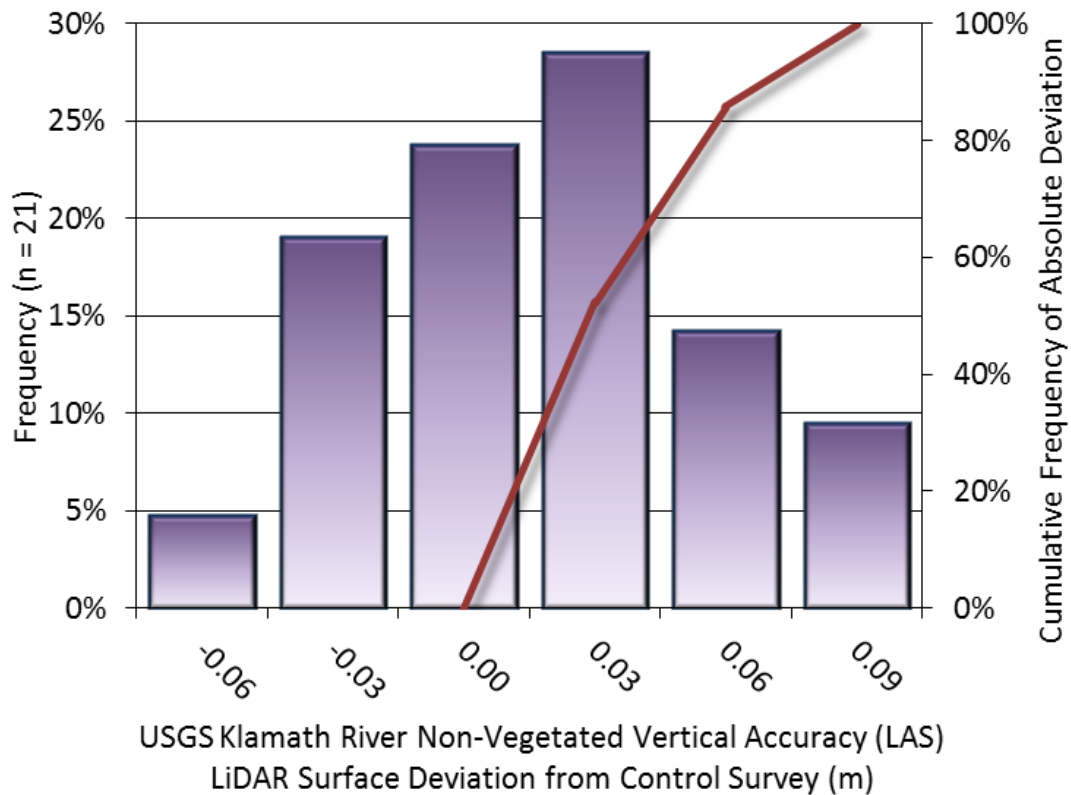
**Figure 12: Frequency histogram for lidar surface deviation from ground check point values as compared to the unclassified point cloud**
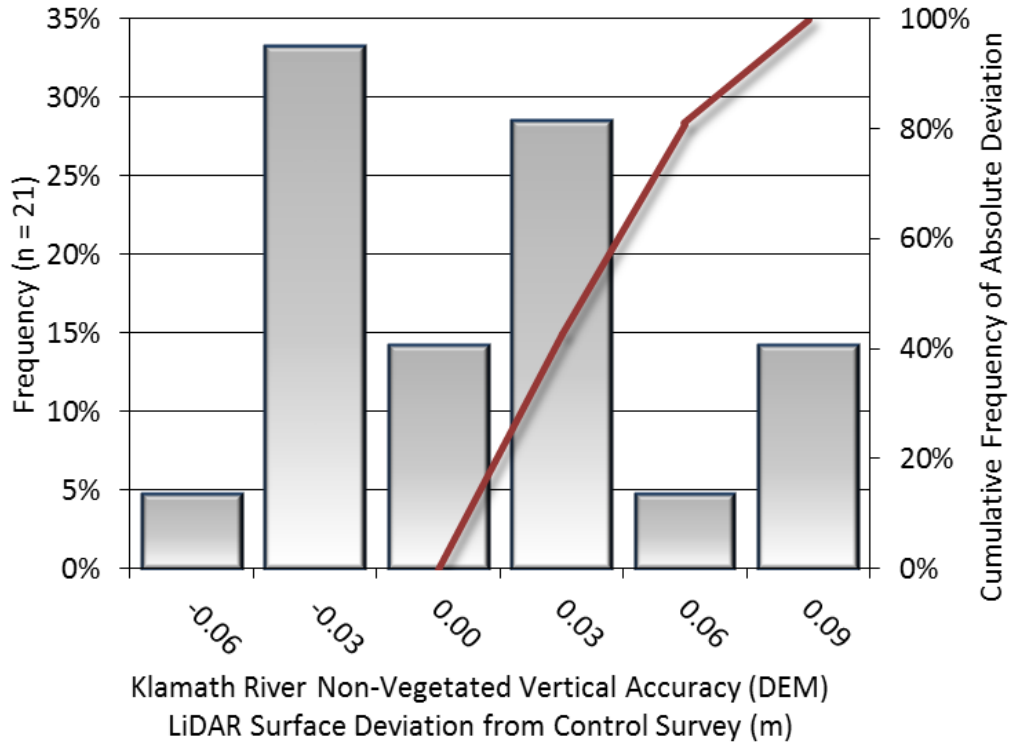
**Figure 13: Frequency histogram for lidar surface deviation from ground check point values as compared to the bare earth digital elevation model**
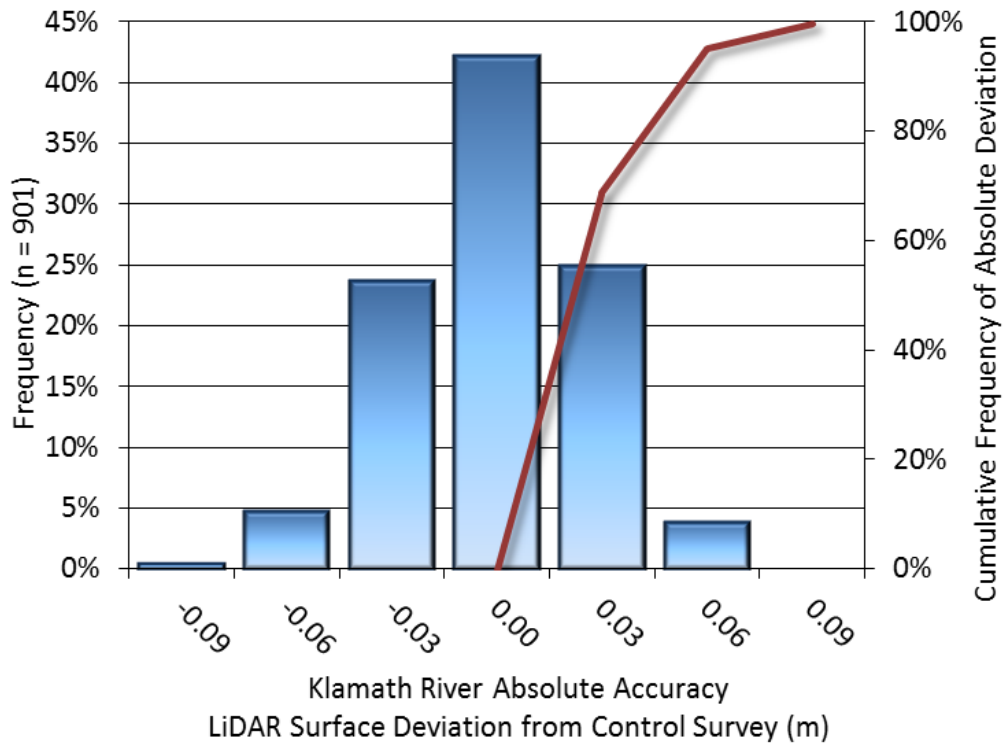


**Figure 14: Frequency histogram for lidar surface deviation ground control point values**

# Lidar Vegetated Vertical Accuracies

QSI also assessed vertical accuracy using Vegetated Vertical Accuracy (VVA) reporting. VVA compares known ground check point data collected over vegetated surfaces using land class descriptions. Check points are compared to the gridded bare earth surface DEM generated by the ground classified lidar points. VVA is evaluated at the 95th percentile. For the Klamath River survey, 9 ground check points were collected over vegetated surfaces, with resulting vegetated vertical accuracy of 0.163 meters at the 95th percentile as compared to the gridded bare earth surface. (Table 18, Figure 15).

**Table 18: Vegetated Vertical Accuracy for the Klamath River Project**

| Vegetated Vertical Accuracy (VVA) | |
|---|---|
| Sample | 9 points |
| Average Dz | 0.071 m |
| Median | 0.075 m |
| RMSE | 0.103 m |
| Standard Deviation (1σ) | 0.079 m |
| 95th Percentile | 0.163 m |
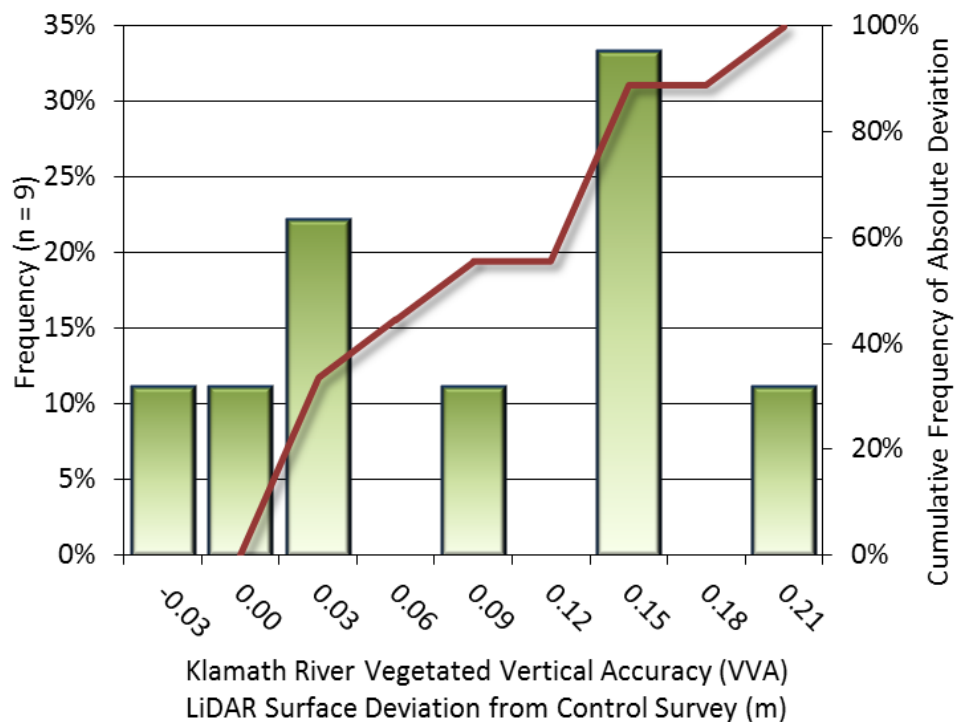


**Figure 15: Frequency histogram for lidar surface deviation from all land cover class point values (VVA)**

# Lidar Bathymetric Vertical Accuracies

Bathymetric (submerged or along the water's edge) check points were also collected in order to assess the submerged surface vertical accuracy. Assessment of the bathymetric checkpoints was performed against the triangulated surface generated by the bathymetric lidar point cloud. Assessment of 103 submerged bathymetric check points resulted in a vertical accuracy of 0.089 meters, while assessment of 78 wetted edge check points resulted in a vertical accuracy of 0.085 meters, with 95% confidence (Figure 16 and Figure 17). Table 19 below presents bathymetric accuracy results and also includes summary statistics for the submerged bathymetric check points at various depth ranges.

**Table 19: Bathymetric Vertical Accuracy**

| Bathymetric Vertical Accuracy for Check Points at Indicated Depth | | | | | | | |
|---|---|---|---|---|---|---|---|
| | Submerged Check Points | | | | | | Wetted Edge Check Points |
| | 0 – 0.25 m | 0.25 – 0.5 m | 0.5 – 0.75 m | 0.75 – 1.0 m | > 1.0 m | Cumulative | |
| **Sample** | 17 points | 28 points | 31 points | 22 points | 5 points | 103 points | 78 points |
| **Average DZ** | -0.031 m | -0.011 m | 0.003 m | 0.001 m | 0.024 m | -0.006 m | -0.005 m |
| **Median** | -0.032 m | -0.021 m | -0.011 m | -0.019 m | 0.013 m | -0.019 m | -0.006 m |
| **RMSE** | 0.048 m | 0.040 m | 0.043 m | 0.052 m | 0.049 m | 0.045 m | 0.043 m |
| **Standard Deviation (1σ)** | 0.037 m | 0.039 m | 0.043 m | 0.053 m | 0.047 m | 0.045 m | 0.043 m |
| **95% confidence** | 0.093 m | 0.079 m | 0.084 m | 0.102 m | 0.095 m | 0.089 m | 0.085 m |
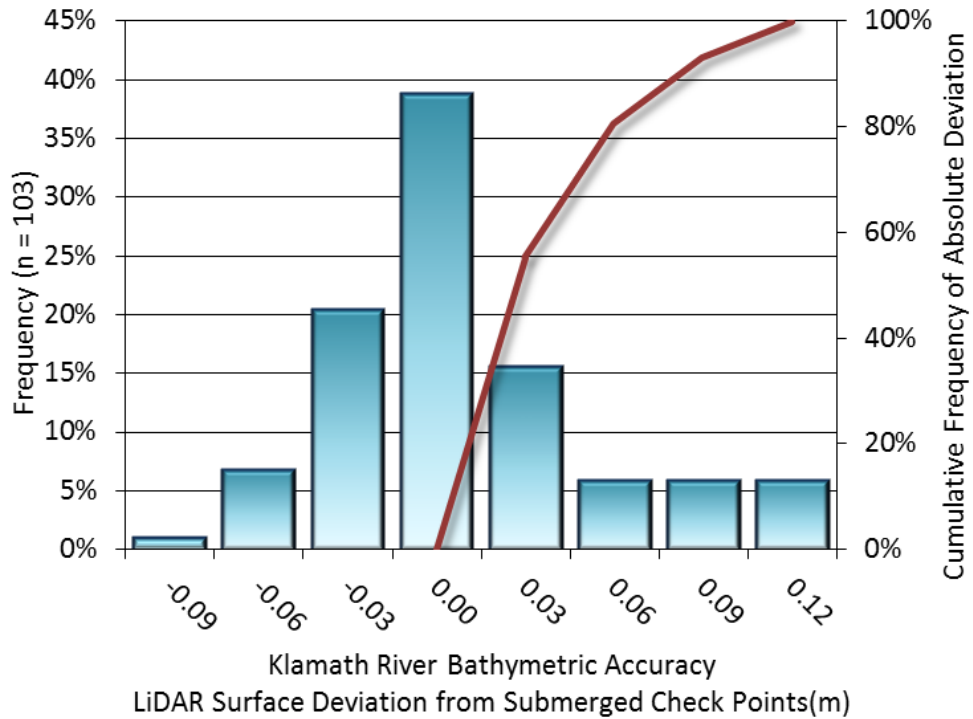
**Figure 16: Frequency histogram for lidar surface deviation from bathymetric check point values**
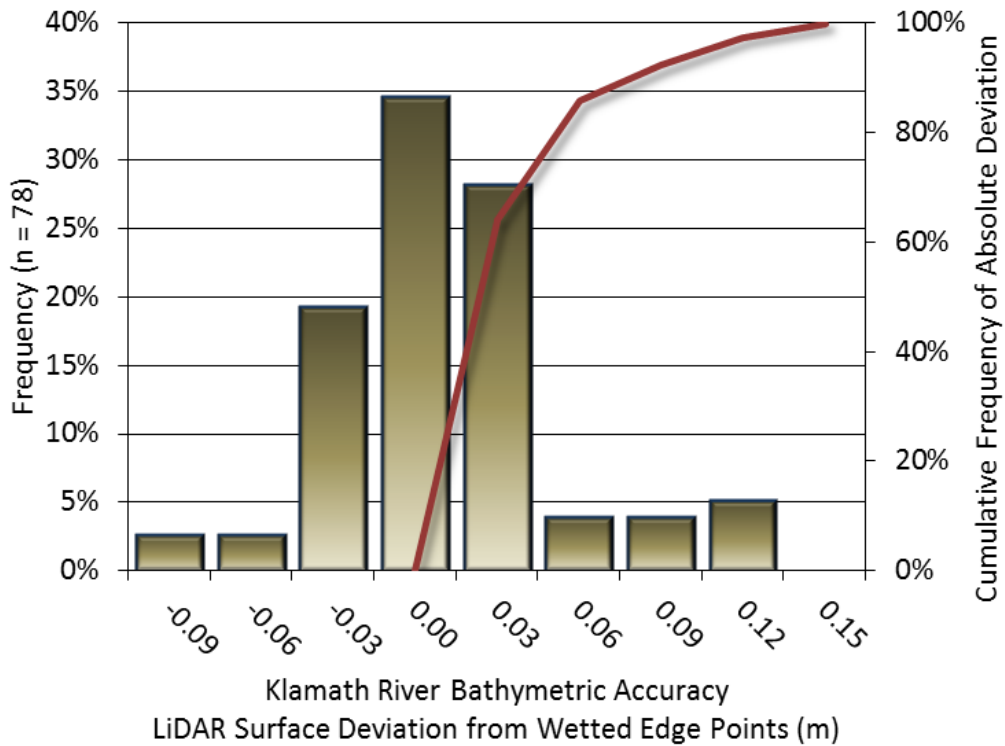


**Figure 17: Frequency histogram for lidar surface deviation from wetted edge check point values**

# Lidar Relative Vertical Accuracy

Relative vertical accuracy refers to the internal consistency of the data set as a whole: the ability to place an object in the same location given multiple flight lines, GPS conditions, and aircraft attitudes. When the lidar system is well calibrated, the swath-to-swath vertical divergence is low (<0.10 meters). The relative vertical accuracy was computed by comparing the ground surface model of each individual flight line with its neighbors in overlapping regions. The average (mean) line to line relative vertical accuracy for the Klamath River lidar project was 0.045 meters (Table 20, Figure 18).

**Table 20: Relative accuracy results**

| Relative Accuracy | |
|---|---|
| **Sample** | 1,328 surfaces |
| **Average** | 0.045 m |
| **Median** | 0.046 m |
| **RMSE** | 0.050 m |
| **Standard Deviation (1σ)** | 0.014 m |
| **1.96σ** | 0.028 m |
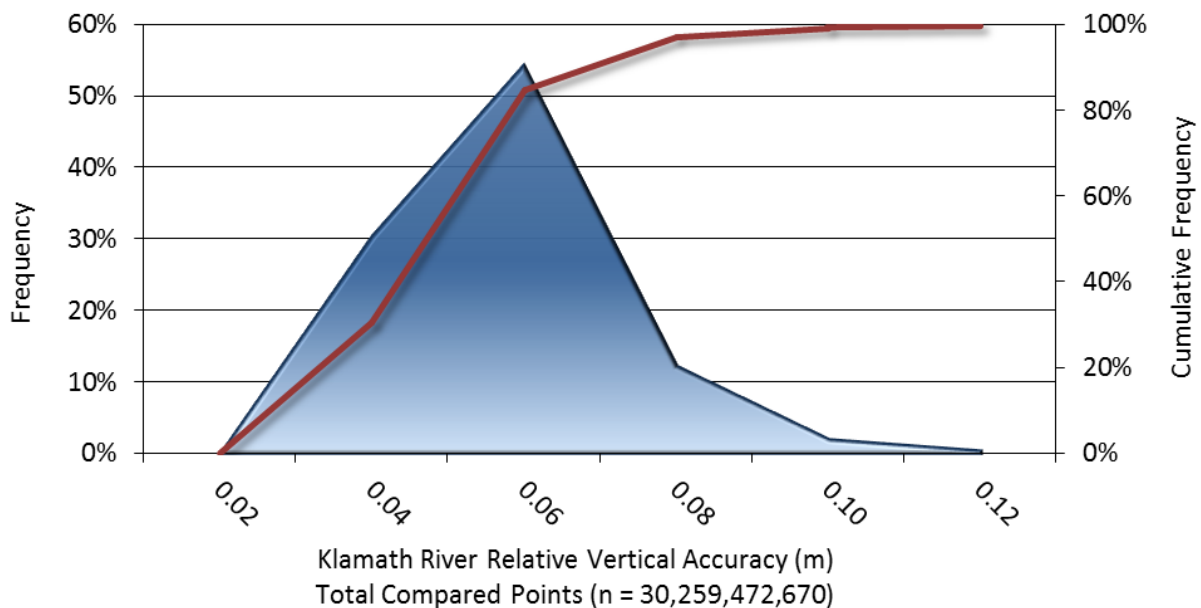


**Figure 18: Frequency plot for relative vertical accuracy between flight lines**

# Digital Imagery Accuracy Assessment

Image accuracy was measured by independent air target check points withheld from the aerial triangulation procedure. Check points were identified in the orthophotos and the displacement was recorded for further statistical analysis.

The circular standard error (CSE) for the Klamath River site is 0.102 meters; the circular standard error was approximated based on the FGDC National Standard for Spatial Data Accuracy (NSSDA) for horizontal accuracy[3]. The CSE (at 95% standard) was computed as follows:

where $RMSE_x = RMSE_y$: $CSE = 1.7308 * RMSE_{xy}$

Table 21 presents the complete photo accuracy statistics.

**Table 21: Orthophotography accuracy statistics for Klamath River**

| Klamath River Photo Accuracy | | | | |
|---|---|---|---|---|
| | | Check Points$_x$ | Check Points$_y$ | Check Points$_{xy}$ |
| Count | | n = 21 | | |
| Mean | *m* | 0.005 | 0.044 | 0.045 |
| RMSE | *m* | 0.070 | 0.072 | 0.100 |
| 1σ | *m* | 0.071 | 0.058 | 0.092 |
| 1.96σ | *m* | 0.140 | 0.114 | 0.180 |

---

[3] Federal Geographic Data Committee, Geospatial Positioning Accuracy Standards (FGDC-STD-007.3-1998). Part 3: National Standard for Spatial Data Accuracy, Appendix 3-A, page 3-10. http://www.fgdc.gov/standards/projects/FGDC-standards-projects/accuracy/part3/chapter3

# Analytical Aerial Triangulation Report

## Overview

Aerotriangulation was performed in one block to support photogrammetric mapping efforts of the Klamath River. The block consisted of 67 flight lines and 1,781 images flown at a scale of 1:1,200 between June 8 and 23, 2018 (Figure 19). Adjustments were made to ground control established by QSI and GMA referencing UTM Zone 10N, NAD83(2011) horizontal datum and NAVD 1988 vertical datum (Geoid12b). Digital imagery along with ground control and camera calibration data were used as input to Inpho's Match AT softcopy photogrammetry program. The digital cameras utilized were an UltraCam XP and and UltraCam Falcon. Of the 121 total surveyed air target points, 48 were used for aerial triangulation, 21 were withheld from the block adjustment as check points for accuracy assessment and 52 were designated as extraneous because of close proximity to neighboring air target points. Extraneous points are ATPs surveyed over the same ground feature, for example of the four ATPs surveyed at each corner of a stop bar only one would be used for control purposes. This redundancy helps when reviewing the orthos during QAQC and serves as a failsafe in the case that a ground control point fails precision requirements.
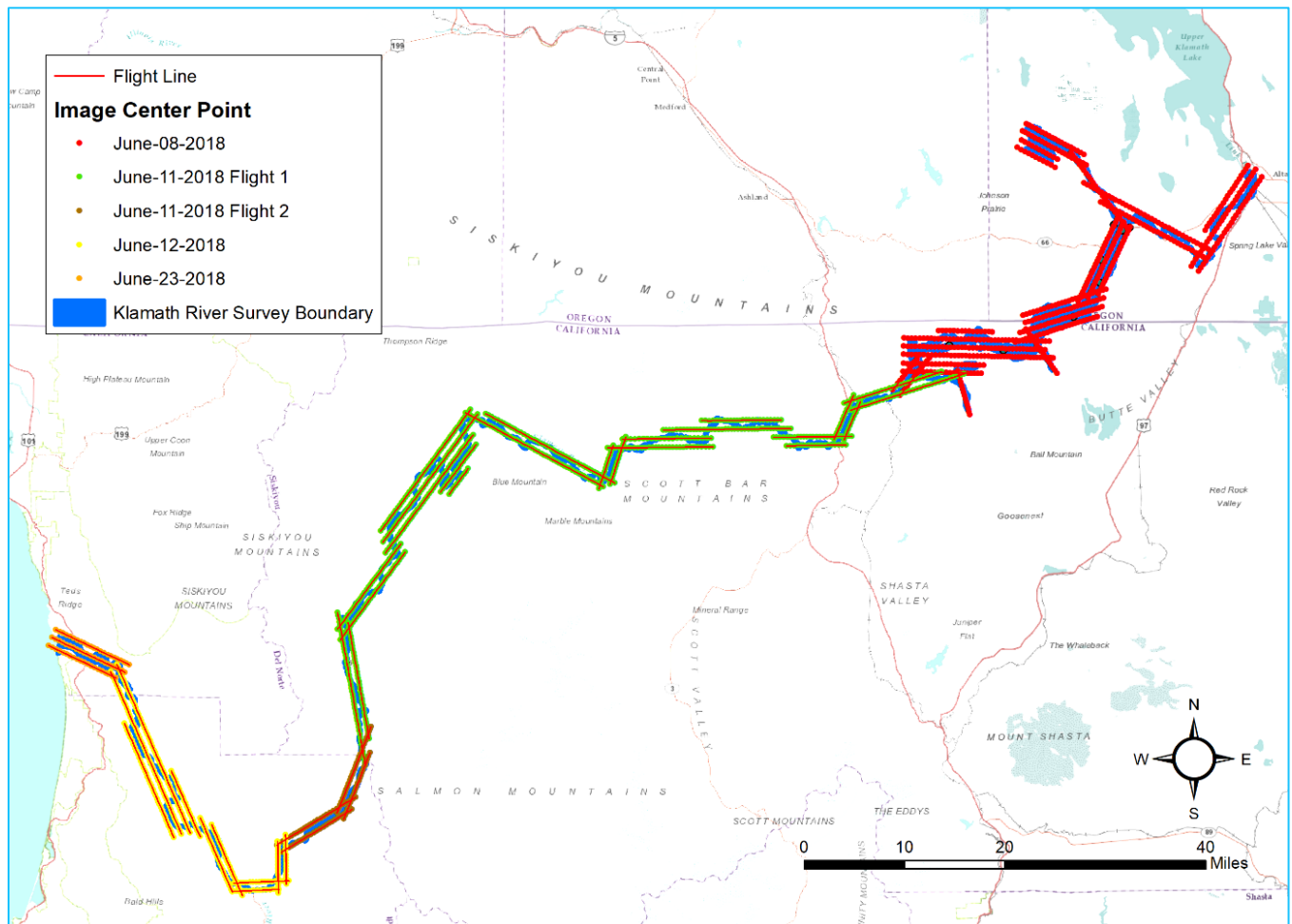


**Figure 19: Klamath River photo flight diagram**

# Control Points

Air target points used in the aerial triangulation adjustment are listed with their coordinates and residuals in Table 22, RMSE values can be found in Table 23.

**Table 22: Location and residuals of air target points used as control for aerial triangulation adjustment**

| | Control Point Coordinates - 48 Total Points | | | Control Point Residuals | | |
|---|---|---|---|---|---|---|
| Point ID | X (m) | Y (m) | Z (m) | X (m) | Y (m) | Z (m) |
| 1075 | 580246.483 | 4665354.503 | 1161.097 | -0.030 | -0.067 | -0.084 |
| 1093 | 581392.132 | 4665817.716 | 1187.552 | 0.007 | 0.004 | -0.033 |
| 5009 | 561156.585 | 4646145.287 | 798.080 | -0.023 | 0.035 | 0.144 |
| 5026 | 572365.872 | 4651530.767 | 1028.460 | 0.025 | -0.043 | 0.004 |
| 5027 | 576569.545 | 4656941.306 | 1288.734 | 0.046 | 0.005 | 0.230 |
| 5335 | 552415.234 | 4646994.637 | 718.935 | -0.026 | 0.002 | -0.204 |
| AT002 | 599071.311 | 4667696.294 | 1248.811 | -0.003 | 0.019 | -0.028 |
| AT004 | 591891.242 | 4658742.964 | 1265.171 | -0.019 | -0.020 | 0.252 |
| AT007 | 575374.421 | 4670901.206 | 1258.952 | -0.004 | 0.016 | 0.008 |
| AT008 | 573228.852 | 4677395.865 | 1385.610 | 0.017 | 0.000 | 0.119 |
| AT009 | 565319.538 | 4681951.869 | 1518.179 | -0.006 | 0.019 | 0.062 |
| AT014 | 552871.665 | 4641977.710 | 817.752 | 0.023 | -0.054 | -0.205 |
| AT016 | 544750.245 | 4640776.959 | 661.250 | 0.089 | 0.009 | -0.208 |
| AT017 | 540734.504 | 4638593.410 | 658.662 | -0.008 | 0.043 | 0.239 |
| AT022 | 525441.937 | 4633423.212 | 581.357 | -0.019 | 0.011 | 0.088 |
| AT023 | 521730.135 | 4635102.013 | 567.099 | 0.022 | -0.013 | 0.052 |
| AT025 | 512495.447 | 4631521.269 | 532.292 | 0.003 | -0.064 | -0.112 |
| AT027 | 500218.475 | 4630225.762 | 493.948 | 0.021 | 0.016 | -0.076 |
| AT028 | 497008.546 | 4625078.904 | 478.125 | -0.001 | -0.007 | -0.147 |
| AT030 | 490387.774 | 4628693.847 | 454.955 | -0.010 | -0.018 | 0.159 |
| AT032 | 483547.580 | 4632357.392 | 417.449 | -0.016 | 0.005 | 0.036 |
| AT033 | 474363.123 | 4634108.597 | 383.205 | -0.018 | 0.030 | -0.055 |
| AT034 | 472092.659 | 4627258.100 | 532.925 | 0.023 | -0.021 | 0.006 |
| AT037 | 463544.929 | 4619188.517 | 306.006 | -0.010 | 0.020 | -0.042 |
| AT038 | 462519.358 | 4612294.688 | 280.743 | -0.010 | -0.001 | 0.004 |
| AT040 | 455386.776 | 4602482.205 | 237.672 | 0.015 | 0.018 | -0.100 |
| AT041 | 456110.131 | 4597462.614 | 223.363 | -0.013 | -0.022 | 0.069 |
| AT043 | 459159.267 | 4581173.715 | 202.519 | 0.005 | 0.010 | 0.035 |
| AT044 | 456393.420 | 4573572.360 | 180.134 | -0.007 | 0.005 | -0.067 |
| AT046 | 444942.081 | 4565484.052 | 122.927 | 0.043 | 0.026 | -0.017 |
| AT047 | 444052.501 | 4561069.860 | 116.054 | 0.023 | -0.003 | -0.062 |
| AT049 | 431385.575 | 4570153.846 | 65.817 | 0.019 | -0.010 | -0.185 |
| AT050 | 435335.010 | 4566485.469 | 100.528 | -0.010 | 0.011 | -0.168 |
| AT052 | 417500.811 | 4595810.800 | 21.706 | 0.010 | 0.021 | -0.213 |
| AT055 | 411580.803 | 4601415.413 | 7.829 | -0.003 | 0.001 | -0.075 |

| Control Point Coordinates - 48 Total Points | | | | Control Point Residuals | | |
|---|---|---|---|---|---|---|
| Point ID | X (m) | Y (m) | Z (m) | X (m) | Y (m) | Z (m) |
| AT057 | 508727.111 | 4632525.991 | 515.498 | 0.019 | 0.041 | -0.025 |
| AT058 | 555117.892 | 4644532.126 | 946.111 | -0.045 | 0.027 | 0.080 |
| AT003_QA | 592835.228 | 4666303.697 | 1259.790 | -0.008 | -0.006 | -0.145 |
| AT005_QA | 588623.635 | 4664689.633 | 1252.052 | 0.001 | 0.013 | -0.041 |
| AT017_QA | 540736.572 | 4638599.999 | 658.501 | -0.213 | 0.057 | 0.212 |
| AT024_QA | 515133.107 | 4635371.713 | 541.525 | -0.040 | 0.007 | 0.120 |
| AT029_QA | 469028.988 | 4627934.606 | 350.803 | 0.000 | -0.004 | 0.005 |
| AT062_QA | 533920.008 | 4631235.505 | 630.637 | -0.044 | -0.063 | 0.020 |
| AT064_QA | 536101.690 | 4638883.225 | 686.085 | 0.313 | 0.009 | -0.186 |
| AT065_QA | 538026.537 | 4638582.116 | 650.273 | -0.130 | -0.025 | 0.057 |
| AT069_QA | 596905.761 | 4664028.129 | 1247.222 | 0.008 | 0.002 | 0.065 |
| AT071_QA | 600195.096 | 4671848.831 | 1257.494 | -0.012 | -0.014 | -0.138 |
| AT072_QA | 600620.188 | 4675057.391 | 1246.444 | 0.015 | 0.006 | 0.349 |

**Table 23: RMSE for air target points used as control for aerial triangulation adjustment**

| Control Point RMSE - 48 Total Points | | |
|---|---|---|
| meters | | |
| X | Y | Z |
| 0.062 | 0.027 | 0.132 |

## Check Points

Air target check points withheld from the aerial triangulation adjustment are listed with their coordinates and residuals in Table 24, RMSE values can be found in Table 25.

**Table 24: Location and residuals of air target check points withheld from aerial triangulation adjustment**

| Check Point Coordinates - 21 Total Points | | | | Check Point Residuals | | |
|---|---|---|---|---|---|---|
| Point ID | X (m) | Y (m) | Z (m) | X (m) | Y (m) | Z (m) |
| 1076 | 580244.841 | 4665370.441 | 1160.651 | 0.018 | 0.052 | -0.122 |
| 1079 | 578849.379 | 4666257.977 | 1175.755 | -0.077 | 0.006 | -0.192 |
| 5000 | 576792.358 | 4660636.165 | 1021.605 | 0.134 | -0.133 | 0.273 |
| AT001 | 600186.965 | 4674919.461 | 1247.069 | 0.013 | 0.055 | 0.397 |
| AT015 | 546271.121 | 4642338.107 | 669.109 | 0.082 | -0.022 | -0.463 |
| AT020 | 535477.504 | 4633740.482 | 630.503 | -0.098 | -0.158 | -0.034 |
| AT021 | 531653.584 | 4631401.972 | 608.771 | -0.175 | -0.072 | 0.118 |
| AT024 | 515117.153 | 4635367.644 | 541.726 | -0.047 | 0.127 | 0.171 |
| AT026 | 502924.637 | 4630194.929 | 501.561 | 0.069 | 0.109 | -0.140 |
| AT035 | 468403.961 | 4626575.651 | 333.763 | 0.018 | -0.033 | 0.008 |
| AT039 | 458715.150 | 4607100.629 | 260.670 | 0.074 | -0.026 | -0.142 |

| Check Point Coordinates - 21 Total Points | | | | Check Point Residuals | | |
|---|---|---|---|---|---|---|
| Point ID | X (m) | Y (m) | Z (m) | X (m) | Y (m) | Z (m) |
| AT051 | 428702.727 | 4574749.439 | 67.775 | 0.071 | 0.101 | -0.490 |
| AT054 | 413363.330 | 4598025.829 | 13.209 | 0.111 | -0.101 | -0.575 |
| AT020_QA | 535468.364 | 4633745.537 | 630.727 | -0.131 | -0.155 | -0.065 |
| AT035_QA | 468401.353 | 4626576.875 | 333.586 | -0.070 | -0.021 | -0.118 |
| AT036_QA | 468773.808 | 4627537.369 | 351.861 | -0.070 | 0.036 | -0.174 |
| AT059_QA | 468841.193 | 4627388.338 | 351.681 | 0.081 | 0.011 | -0.154 |
| AT060_QA | 535367.015 | 4633787.623 | 631.614 | -0.083 | -0.079 | -0.054 |
| AT061_QA | 535361.853 | 4633783.398 | 631.859 | -0.024 | -0.211 | -0.057 |
| AT068_QA | 539626.172 | 4638509.520 | 648.417 | -0.112 | -0.082 | 0.286 |
| AT070_QA | 595231.229 | 4666776.222 | 1247.040 | -0.030 | -0.001 | -0.013 |

**Table 25: RMSE for air target points withheld from aerial triangulation adjustment**

| Check Point RMSE - 21 Total Points | | |
|---|---|---|
| meters | | |
| X | Y | Z |
| 0.086 | 0.095 | 0.250 |

# Adjusted Exterior Orientation Parameters

The refined camera position and attitude parameters for each image event can be found in the provided Klamath_River_Photo_Flight_Index.xlsx deliverable.

Quantum Spatial, Inc. provided lidar services for the Klamath River project as described in this report.

I, Steve Miller, have reviewed the attached report for completeness and hereby state that it is a complete and accurate report of this project.

_(signature)_        Jul 26, 2019

Steve Miller
Project Manager
Quantum Spatial, Inc.

I, Evon P. Silvia, PLS, being duly registered as a Professional Land Surveyor in and by the states of Oregon and California, hereby certify that the methodologies, static GNSS occupations used during airborne flights, and ground survey point collection were performed using commonly accepted Standard Practices. QSI field work conducted for this report was conducted between May 30 and June 12, 2018.

Accuracy statistics shown in the Accuracy Section of this Report have been reviewed by me and found to meet the "National Standard for Spatial Data Accuracy".

REGISTERED
PROFESSIONAL
LAND SURVEYOR

_(signature)_ Evon P. Silvia

OREGON
JUNE 10, 2014
EVON P. SILVIA
81104LS

EXPIRES: 06/30/2020

LICENSED LAND SURVEYOR
EVON PETER SILVIA
_(signature)_ Evon P. Silvia
STATE OF CALIFORNIA
9401
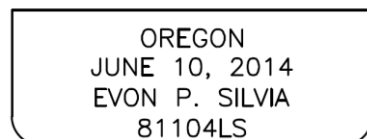
Signed: Jul 26, 2019

Evon P. Silvia, PLS
Quantum Spatial, Inc.
Corvallis, OR 97330
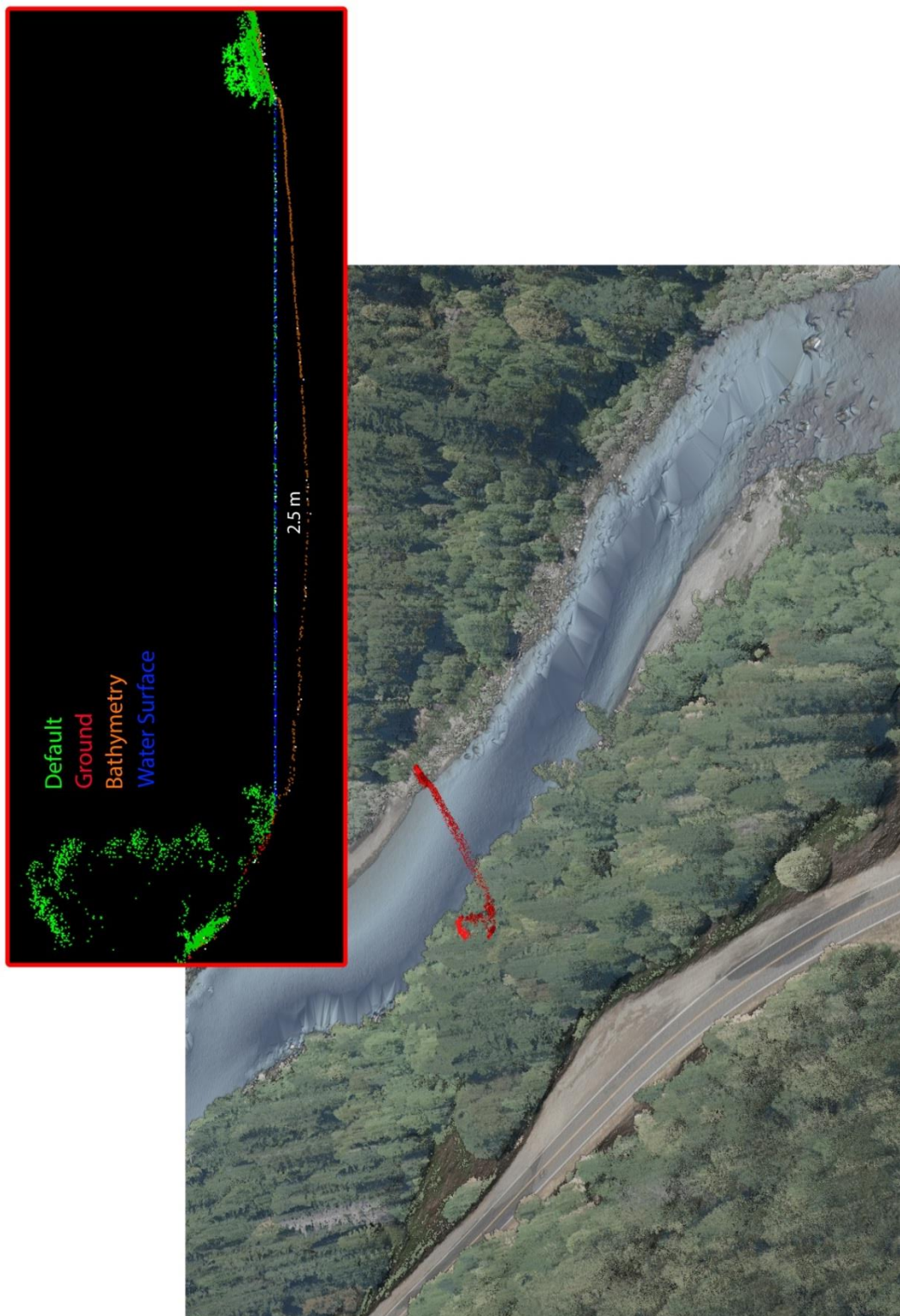
**Figure 20: View of Klamath River near Teneyck Creek, the shaded bare-earth and topobathymetric model and above ground lidar point cloud are draped with 0.15 m ortho imagery.**

**Figure 21: A view looking north along the Klamath River in northern California. This image was created from the lidar bare earth model colored by elevation and overlaid with digital imagery acquired by QSI.**

**1-sigma (σ) Absolute Deviation:**  Value for which the data are within one standard deviation (approximately 68th percentile) of a normally distributed data set.

**1.96 * RMSE Absolute Deviation:**  Value for which the data are within two standard deviations (approximately 95th percentile) of a normally distributed data set, based on the FGDC standards for Non-vegetated Vertical Accuracy (FVA) reporting.

**Accuracy**:  The statistical comparison between known (surveyed) points and laser points. Typically measured as the standard deviation (sigma σ) and root mean square error (RMSE).

> **Absolute Accuracy:**  The vertical accuracy of lidar data is described as the mean and standard deviation (sigma σ) of divergence of lidar point coordinates from ground survey point coordinates. To provide a sense of the model predictive power of the dataset, the root mean square error (RMSE) for vertical accuracy is also provided. These statistics assume the error distributions for x, y and z are normally distributed, and thus we also consider the skew and kurtosis of distributions when evaluating error statistics.

> **Relative Accuracy:**  Relative accuracy refers to the internal consistency of the data set; i.e., the ability to place a laser point in the same location over multiple flight lines, GPS conditions and aircraft attitudes. Affected by system attitude offsets, scale and GPS/IMU drift, internal consistency is measured as the divergence between points from different flight lines within an overlapping area. Divergence is most apparent when flight lines are opposing. When the lidar system is well calibrated, the line-to-line divergence is low (<10 cm).

> **Root Mean Square Error (RMSE):**  A statistic used to approximate the difference between real-world points and the lidar points. It is calculated by squaring all the values, then taking the average of the squares and taking the square root of the average.

**Data Density**:  A common measure of lidar resolution, measured as points per square meter.

**Digital Elevation Model (DEM)**:  File or database made from surveyed points, containing elevation points over a contiguous area. Digital terrain models (DTM) and digital surface models (DSM) are types of DEMs. DTMs consist solely of the bare earth surface (ground points), while DSMs include information about all surfaces, including vegetation and man-made structures.

**Intensity Values**:  The peak power ratio of the laser return to the emitted laser, calculated as a function of surface reflectivity.

**Nadir**:  A single point or locus of points on the surface of the earth directly below a sensor as it progresses along its flight line.

**Overlap**:  The area shared between flight lines, typically measured in percent. 100% overlap is essential to ensure complete coverage and reduce laser shadows.

**Pulse Rate (PR)**:  The rate at which laser pulses are emitted from the sensor; typically measured in thousands of pulses per second (kHz).

**Pulse Returns**:  For every laser pulse emitted, the number of wave forms (i.e., echoes) reflected back to the sensor. Portions of the wave form that return first are the highest element in multi-tiered surfaces such as vegetation. Portions of the wave form that return last are the lowest element in multi-tiered surfaces.

**Real-Time Kinematic (RTK) Survey**:  A type of surveying conducted with a GPS base station deployed over a known monument with a radio connection to a GPS rover. Both the base station and rover receive differential GPS data and the baseline correction is solved between the two. This type of ground survey is accurate to 1.5 cm or less.

**Post-Processed Kinematic (PPK) Survey**:  GPS surveying is conducted with a GPS rover collecting concurrently with a GPS base station set up over a known monument. Differential corrections and precisions for the GNSS baselines are computed and applied after the fact during processing. This type of ground survey is accurate to 1.5 cm or less.

**Scan Angle**:  The angle from nadir to the edge of the scan, measured in degrees. Laser point accuracy typically decreases as scan angles increase.

**Native Lidar Density**:  The number of pulses emitted by the lidar system, commonly expressed as pulses per square meter.

**Relative Accuracy Calibration Methodology:**

Manual System Calibration:  Calibration procedures for each mission require solving geometric relationships that relate measured swath-to-swath deviations to misalignments of system attitude parameters. Corrected scale, pitch, roll and heading offsets were calculated and applied to resolve misalignments. The raw divergence between lines was computed after the manual calibration was completed and reported for each survey area.

Automated Attitude Calibration:  All data were tested and calibrated using TerraMatch automated sampling routines. Ground points were classified for each individual flight line and used for line-to-line testing. System misalignment offsets (pitch, roll and heading) and scale were solved for each individual mission and applied to respective mission datasets. The data from each mission were then blended when imported together to form the entire area of interest.

Automated Z Calibration: Ground points per line were used to calculate the vertical divergence between lines caused by vertical GPS drift. Automated Z calibration was the final step employed for relative accuracy calibration.

**Lidar accuracy error sources and solutions:**

| Type of Error | Source | Post Processing Solution |
|---|---|---|
| GPS (Static/Kinematic) | Long Base Lines | None |
| | Poor Satellite Constellation | None |
| | Poor Antenna Visibility | Reduce Visibility Mask |
| Relative Accuracy | Poor System Calibration | Recalibrate IMU and sensor offsets/settings |
| | Inaccurate System | None |
| Laser Noise | Poor Laser Timing | None |
| | Poor Laser Reception | None |
| | Poor Laser Power | None |
| | Irregular Laser Shape | None |

**Operational measures taken to improve relative accuracy:**

Low Flight Altitude:  Terrain following was employed to maintain a constant above ground level (AGL). Laser horizontal errors are a function of flight altitude above ground (about 1/3000th AGL flight altitude).

Focus Laser Power at narrow beam footprint:  A laser return must be received by the system above a power threshold to accurately record a measurement. The strength of the laser return (i.e., intensity) is a function of laser emission power, laser footprint, flight altitude and the reflectivity of the target. While surface reflectivity cannot be controlled, laser power can be increased and low flight altitudes can be maintained.

Reduced Scan Angle:  Edge-of-scan data can become inaccurate. The scan angle was reduced to a maximum of ±20$^{o}$ from nadir, creating a narrow swath width and greatly reducing laser shadows from trees and buildings.

Quality GPS:  Flights took place during optimal GPS conditions (e.g., 6 or more satellites and PDOP [Position Dilution of Precision] less than 3.0). Before each flight, the PDOP was determined for the survey day. During all flight times, a dual frequency DGPS base station recording at 1 second epochs was utilized and a maximum baseline length between the aircraft and the control points was less than 13 nm at all times.

Ground Survey:  Ground survey point accuracy (<1.5 cm RMSE) occurs during optimal PDOP ranges and targets a minimal baseline distance of 4 miles between GPS rover and base. Robust statistics are, in part, a function of sample size (n) and distribution. Ground survey points are distributed to the extent possible throughout multiple flight lines and across the survey area.

50% Side-Lap (100% Overlap):  Overlapping areas are optimized for relative accuracy testing. Laser shadowing is minimized to help increase target acquisition from multiple scan angles. Ideally, with a 50% side-lap, the nadir portion of one flight line coincides with the swath edge portion of overlapping flight lines. A minimum of 50% side-lap with terrain-followed acquisition prevents data gaps.

Opposing Flight Lines:  All overlapping flight lines have opposing directions. Pitch, roll and heading errors are amplified by a factor of two relative to the adjacent flight line(s), making misalignments easier to detect and resolve.

THIS PAGE INTENTIONALLY LEFT BLANK

# 2018 KLAMATH DAM REMOVAL PROJECT
## TOPOBATHYMETRIC LIDAR & SONAR
## TECHNICAL DATA REPORT

AECOM Project Number 60537920

Prepared for:

**AECOM**
300 Lakeside Drive, Suite 400
Oakland, CA 94612

Prepared by:

**Cort Pryor**

**GMA Hydrology, Inc. (GMA)**
5435 Ericson Way, Suite 1
Arcata, CA 95521
(707) 825-6681

**December, 2018**

# Table of Contents

# EXECUTIVE SUMMARY

In support of the Klamath Hydroelectric Settlement Agreement (KHSA), four PacifiCorp hydropower facilities located in the Klamath River Basin (Iron Gate Dam, Copco No. 1 Dam, Copco No. 2 Dam and J.C. Boyle Dam) were surveyed using topo-bathymetric airborne LiDAR, multibeam sonar, sweep sonar and conventional methods.

This report summarizes the geodetic control, data collection techniques, processing and data integration methodologies, as well as the assessed accuracy of the datasets.

# SURVEYOR'S STATEMENT

I, Benjamin L. Hocker as a licensed land surveyor in the state of Oregon (No. 85654), certify that the airborne LiDAR, multibeam sonar, sweep sonar and terrestrial control survey data within Oregon compiled by GMA Hydrology, Inc. in partnership with Geomatics Data Solutions, Inc. follows commonly accepted standard practices. Accuracy statistics shown were tested to meet a 0.61 (ft) $RMSE_z$ Vertical Accuracy Class based on ASPRS Positional Accuracy Standards for Digital Geospatial Data (2014). The 2018 Klamath River Survey Report (GMA Hydrology, Inc., 2018) documents data collection methods, processing, and data integration methods.

REGISTERED
PROFESSIONAL
LAND SURVEYOR

OREGON
JUNE 12, 2013
BENJAMIN LANE HOCKER
85654

RENEWS DATE: June 30, 20 19

I, David T. Edson as a licensed land surveyor in the state of California (No. 4974), certify that the airborne LiDAR, multibeam sonar, sweep sonar and terrestrial control survey data within California compiled by GMA Hydrology, Inc. in partnership with Geomatics Data Solutions, Inc. follows commonly accepted standard practices. Accuracy statistics shown were tested to meet a 0.61 (ft) $RMSE_z$ Vertical Accuracy Class based on ASPRS Positional Accuracy Standards for Digital Geospatial Data (2014). The 2018 Klamath River Survey Report (GMA Hydrology, Inc., 2018) documents data collection methods, processing, and data integration methods.

LICENSED LAND SURVEYOR
DAVID T. EDSON
No. 4974
STATE OF CALIFORNIA

12/3/2018

# INTRODUCTION

## Survey Area

The project area includes the Klamath River and four reservoirs that straddle the Oregon and California border: John C. Boyle Reservoir located in southern Oregon near the township of Keno and Copco 1, Copco 2 and Iron Gate Reservoirs in Siskiyou County, California (Figure 1).

GMA Hydrology, Inc. (GMA) and Geomatics Data Solutions, Inc. (GDS) performed all terrestrial and hydrographic surveys. Airborne surveys were conducted by Quantum Spatial, Inc. (QSI) under contract with GMA.

Data acquisition occurred between February 08, 2018 and August 09, 2018. Acquisition dates and area surveyed, according to survey source, are show in Table 1.

### Table 1. Acquisition Dates and Area Surveyed

| Data Type | Survey Area (sq km) | Acquisition Dates |
|---|---|---|
| LiDAR | 108 | June 11 through June 13, 2018 |
| Bathymetric LiDAR | 1.27 | June 11 through June 13, 2018 |
| Multibeam | 7.59 | February 8, 2018 through 8-Aug-18 |
| Sweep | 0.56 | May 9-10 & 29-30, 2018 |
| GNSS RTK | 0.001 | August 9, 2018 |
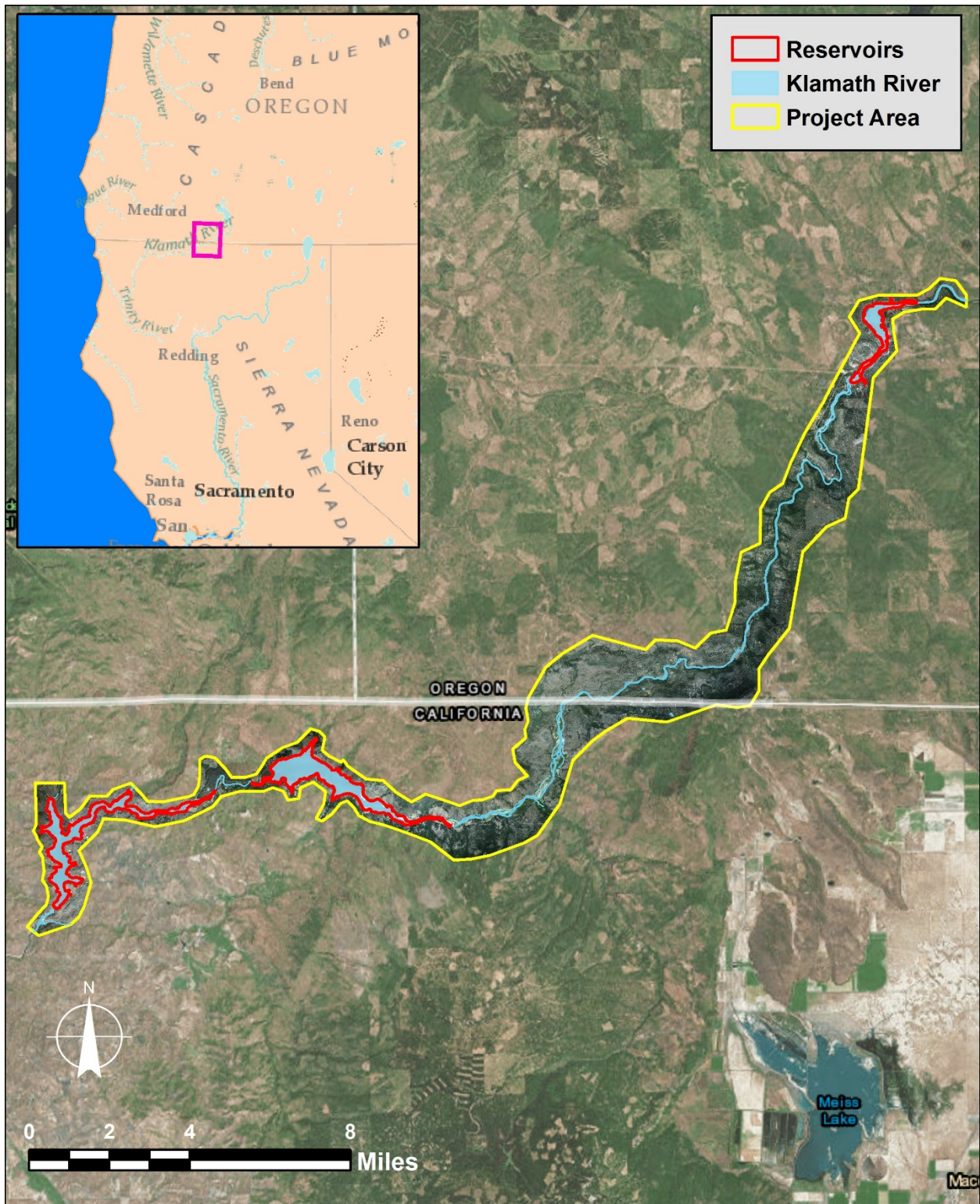
**Figure 1. Klamath River Survey Area Overview**

## DATA ACQUISITION
Equipment specifications can be found in Appendix B.

### Geodetic Control
GMA and GDS established five new control stations and occupied 8 existing stations in the survey area using static Global Navigation Satellite Systems (GNSS) network survey techniques. Trimble R10 and R8 model 3 GNSS receivers were configured to record raw multiple frequency, multiple constellation observables at a rate of 1 Hz. Multiple observations with independent baselines were obtained between existing published NGS control, recovered control from previous LiDAR and imagery projects, and newly set monumentation. Fixed height tripods were used to minimize antenna setup errors. QSI utilized two additional monuments for conducting airborne data acquisition.

The horizontal datum is NAD83 (2011) Epoch 2010.0 and the vertical datum is NAVD88 using GEOID12B. Data are projected in Universal Transverse Mercator, Zone 10 in meters (m).

### LiDAR Surveys
QSI was contracted by GMA to collect topo-bathymetric Light Detection and Ranging (LiDAR) data and digital imagery. The LiDAR survey was accomplished using a Riegl VQ-880-G green laser system mounted in a Bell 206L-3 Rotorcraft. Full details on LIDAR acquisition is described in *Klamath_Reservoirs_Topobathymetric_LiDAR_Report – signed,* submitted under a separate cover.

### Sonar Surveys
GMA and GDS worked in partnership to conduct bathymetric surveys at the four reservoir sites. Two vessels and four sonar systems were utilized during survey operations, as detailed in Table 2.

GDS-Cari (Figure 2) and GMA-Jet are both aluminum hull jet boats fitted with over the side pole mounted multibeam sonar systems. GMA- Jet was also configured with a Ross Laboratories 875-8 portable hydrographic sonar sweep system (Figure 3).

**Table 2: Sonar Systems**

| Survey Area | Vessel | Major Components |
|-------------|--------|------------------|
| John C Boyle | GDS-Cari<br>GMA-Jet | Reson SeaBat T20-P Multibeam<br>Ross 875 8-Channel Sweep |
| Copco 1 | GMA-Jet<br>GDS-Cari | Reson SeaBat T20-P Multibeam<br>Reson SeaBat T20-P Multibeam |
| Copco 2 | GMA-Jet | Norbit iWBMS STX Multibeam |
| Iron Gate | GMA-Jet<br>GDS-Cari | Norbit iWBMSc Multibeam<br>Reson SeaBat T20-P Multibeam |

**Figure 2. GDS-Cari Configured with Pole Mounted Reson T20-P Multibeam Sonar**



**Figure 3. GMA-Jet Configured with Ross 875-8 Sweep Sonar**

## Multibeam Surveys

The multibeam sonar surveys were conducted with a Reson SeaBat T20-P and two different versions of the Norbit iWBMS sonar system. The systems were deployed on the GDS Cari platform well as the GMA Jet boat. Applanix POS/MV inertial navigation systems were used to position and orient the sonar data with auxiliary Trimble R10 and R8 model 3 GNSS receivers for positioning system redundancy and QA/QC. The sonar, inertial, and positioning data were stored on an on-board computer running Applanix and Teledyne PDS survey software. A shore-based Trimble R8 Model 3 GNSS receiver broadcasted Real Time Kinematic (RTK) GNSS positioning corrections to the survey vessels via UHF radio link (Figure 4). Raw GNSS observables were also recorded at the base and vessel for post-processing. Surface sound speed was measured at the sonar head during acquisition by an AML sound speed probe. Sound speed profiles were measured over the full depth of the project area using an AML MinosX profiler.

Proper system operation was calibrated and verified using industry standard position checks, bar checks and patch tests. Crosslines were also collected to verify sonar accuracy and provide an independent check for LiDAR and sweep data.

## Sweep Sonar Surveys

The sonar sweep survey was conducted using a portable multi-channel sonar sweep system. The GMA jet boat was equipped with a Ross Laboratories 875-8 portable hydrographic sonar sweep system, Trimble SPS852/552H GNSS receiver heading bundle, and a Honeywell HMR 3000 attitude sensor. A shore-based Trimble R8 Model 3 GNSS receiver broadcasted Real Time Kinematic (RTK) GNSS positioning corrections to the survey vessels via UHF radio link (Figure 4). Raw GNSS observables were also recorded at the base and vessel for post-processing. The sonar data, RTK GNSS data, and attitude data were combined in a ruggedized laptop computer running Hypack hydrographic surveying software. Sound speed profiles were acquired using a YSI CastAway CTD and an AML BaseX.



**Figure 4. GNSS Base Station**

The control points used for sonar surveys at each reservoir are presented in Table 3.

**Table 3. Control Coordinates on NAD83 (2011) Epoch 2010.0**

| Control Point | Latitude | Longitude | Ellipsoid Height (m) | Survey Area |
|---|---|---|---|---|
| **GMA-200** | N42°07'21.97179" | W122°02'52.79449" | 1136.533 | John C Boyle Reservoir |
| **GMA-202** | N41°58'25.76728" | W122°17'55.95491" | 772.760 | Copco Reservoirs |
| **GMA-203** | N41°57'50.65426" | W122°25'49.06258" | 731.917 | Iron Gate Reservoir |

## Ground Surveys

### Topography

Ground topographic surveys were performed in areas where sonar and topo-bathymetric LiDAR acquisition were not possible. The topographic survey area consisted of a small region of the Copco 2 reservoir about 70 meters downstream of the Copco No. 1 dam. The survey was conducted using Trimble R8 Model 3 and R10 receivers.

### Ground Survey Check Points

GMA, GDS, and QSI collected ground survey check points (GSCP) using RTK, post-processed kinematic (PPK) and fast-static (FS) survey techniques. Multiple frequency, survey grade Trimble GNSS receivers were used as base and rovers for all surveys (models R10, R8-2, R8-3, and R7). Base station receivers were setup on control monuments to broadcast a kinematic correction to rover receivers as well as record raw observables for post-processing. In General GSCP measurements were made during periods with a Position Dilution of Precision (PDOP) of ≤ 3.0 with at least six satellites in view of the stationary and roving receivers. When collecting RTK and PPK data, the rover records data while stationary for five seconds, then calculates the pseudorange position using at least three one-second epochs. FS surveys record observations for up to fifteen minutes on each GSCP in order to support longer baselines for post-processing. Relative errors for any GSCP position must be less than 1.5 cm horizontal and 2.0 cm vertical in order to be accepted.

GSCPs were collected in areas where good satellite visibility was achieved on varying surface types and slopes. GSCPs were distributed over the project area, however distribution of GSCPs depended on ground access constraints and monument locations and may not be equitably distributed throughout the study area.

## DATA PROCESSING

### Geodetic Control

Raw GNSS observables were post processed with precise ephemeris files in Trimble Business Center version 4.00 software. A constrained least squares adjustment was performed to determine final coordinates. Coordinates for all monuments are shown in Appendix A-1.

## Topo-Bathymetric LiDAR

Upon completion of data acquisition, QSI processing staff initiated a suite of automated and manual techniques to process the data into the requested deliverables. Processing tasks included GNSS control computations, smoothed best estimate trajectory (SBET) calculations, kinematic corrections, calculation of laser point position, sensor and data calibration for optimal relative and absolute accuracy, and LIDAR point classification.

Riegl's RiProcess software was used to facilitate bathymetric return processing. Once bathymetric points were differentiated, they were spatially corrected for refraction through the water column based on the angle of incidence of the laser. QSI refracted water column points using QSI's proprietary LAS processing software, LAS Monkey. The resulting point cloud data were classified using both manual and automated techniques. Processing methodologies were tailored for the landscape.

Full details on LIDAR processing is described in *Klamath_Reservoirs_Topobathymetric_LiDAR_Report – signed,* submitted under a separate cover.

## Multibeam and Sweep Sonar

Once sonar data collection was complete, GMA processed all sonar data in Caris HIPS version 10. Processing is a combination of manual and automated techniques that are tailored to the deliverables requested by the client. Processing steps included: defining vessel configurations, SBET calculations, converting raw Hypack and PDS data files to HIPS format, applying sound velocity corrections, reviewing and correcting attitude and navigation data, review and editing of raw sounding data, manual and automated filtering as well as merging the attitude, navigation and raw sounding data. Post-processed trajectory from POSPac was applied to enhance positional accuracy and compute Total Propagated Uncertainty (TPU). For multibeam and sweep sonar data, the processed track lines were binned using a Bathymetry Associated with Statistical Error (BASE) Surface type. Multibeam sonar data was binned using the Combined Uncertainty and Bathymetry Estimator (CUBE) algorithm using 25cm resolution. Sweep sonar data was binned using the CUBE algorithm with a 75 cm resolution. Sonar processing workflow is presented in Table 4.

**Table 4. Sweep and Multibeam Beam Sonar Processing Workflow**

| Sonar Processing Step | Software Used |
|---|---|
| Define vessel configuration for the survey. Configuration includes sensor types and models, location of sensors, lever arms, and uncertainties associates with measurements. | Caris HIPS 10.4.2 |
| Convert raw sonar files to HIPS format. Each survey line is converted separately and stored by day. | Caris HIPS 10.4.2 |
| Import delayed heave, SBET and RMS. | Caris HIPS 10.4.2 POSPac 8.2.6633.20855 |
| Apply sound velocity corrections, review navigation, heading, GNSS water levels, and attitude data. | Caris HIPS 10.4.2 |
| Merge processed soundings with navigation, attitude, and GNSS water levels. | Caris HIPS 10.4.2 |
| Generate CUBE surface and continue processing point cloud in subsets. Automated and manual filtered using the surface as a reference. | Caris HIPS 10.4.7 |
| Export final point cloud by survey line for all crosslines and perform various accuracy assessments. | Caris HIPS 10.4.7 ArcMap 10.6 Microsoft Excel |
| Export CUBE surface resampled on Klamath Reservoirs Index to ASCII. | Caris HIPS 10.4.7 |

Relative vertical confidence checks of the multibeam sonar were completed using crosslines and bar checks. Each bar check was conclusive with differences generally 1cm or less. Crosslines acquired throughout the project area were analyzed in Caris HIPS by creating difference surfaces. 25cm resolution CUBE surfaces of the crosslines were subtracted from 25cm resolution surfaces of the main scheme lines for each reservoir (Table 5). Crossline results were reviewed for across-track bias errors (roll offset, speed of sound errors, etc.), gross error (GNSS height), and total vertical uncertainty (TVU).

## Table 5. Klamath River Reservoirs Crossline Comparisons

| Surface Differencing | |
|---|---|
| Minimum | -1.788 m |
| Maximum | 0.940 m |
| Mean | 0.005 m |
| Standard Deviation | 0.048 m |
| Total Count | 4,623,618 |

Significant man-made features were flagged during data processing to ensure the gridded surfaces would represent those least depths (Figure 5).
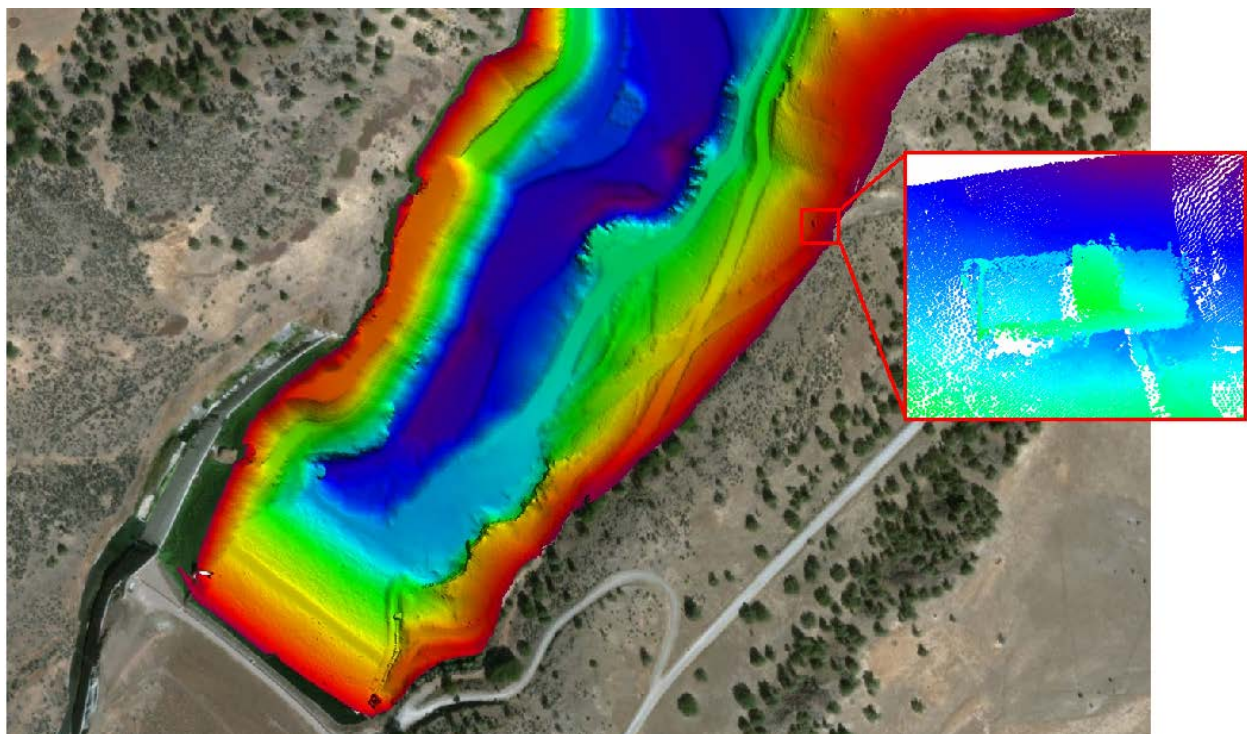


**Figure 5. Truck Located in High Resolution Multibeam at Iron Gate Reservoir**

## Ground Surveys

Topographic and ground survey check point data were processed in Trimble Business Center version 4.00 software. Processing included: verifying values for geodetic control, verifying and modifying rod heights, verifying and modifying point codes, sorting the data to various layers and developing feature breaklines.

## Data Integration and Product Development

The multibeam sonar, sweep sonar and topo-bathymetric LiDAR data were integrated using GeoCue's LP360 4.4 and ArcMap 10.6.  Integration of the data sets included, converting survey data to *.LAS format, updating point classifications (Table 6), developing survey extents by data

**Table 6: LAS File Point Classification**

| Classification Number | Classification Name | Classification Description |
|---|---|---|
| 1 | Default/ Unclassified | Flightline edge clip |
| 2 | Ground | Laser returns that are determined to be ground using automated and manual cleaning algorithms |
| 3 | Low Vegetation | Vegetation between 0.25 and 2 meters |
| 4 | Medium Vegetation | Vegetation between 2 and 5 meters |
| 5 | High Vegetation | Vegetation above 5 meters |
| 7 | Noise | Scattering points and artificial points below the ground surface |
| 9 | NIR Water Surface | NIR laser returns that are determined to be water using automated and manual cleaning algorithms |
| 17 | Bridge | Bridge Decks |
| 40 | Bathy LiDAR | Laser returns determined to be ground within the a wetted region |
| 41 | Green Water Surface | Green laser returns that are determined to be water surface points using automated and manual cleaning algorithms |
| 45 | Water Column | Refracted Riegl sensor returns that are determined to be water using automated and manual cleaning algorithms |
| 71 | GNSS RTK | Ground Survey points that were collected with RTK GPS |
| 80 | Sweep Sonar Binned | Binned sonar returns that were collected with a multi-transducer sonar sweep system |
| 81 | Multibeam Sonar Binned | Binned sonar returns that were collected with a multibeam sonar system |

type, developing buffers for sonar and conventional datasets, developing breaklines, determining absolute accuracy of the dataset, and developing client requested deliverables.  The integration and product development workflow is described in Table 7.

**Table 7:  Data Integration Workflow**

| Data Integration Step | Description |
|---|---|
| Convert and classify data | Convert ASCII files to *.las v1.4 PDRF 6. Classify data based on source. |
| Survey/Data Extents | Develop individual data and survey extents. Develop project extents. |
| Terrain Development and Inspection | Develop terrain using appropriate point classifications, add withheld flag to appropriate classes in areas of overlapping data, apply breaklines developed during conventional survey data processing, and contour.  Add additional breaklines to force correct interpolation of features.  Visually inspect terrain for correct interpolation, additional data flagging and breakline development as needed. |
| Data Accuracy Assessment | Query the terrain dataset with GSCPs.  Develop statistics according to ASPRS Positional Accuracy Standards for Digital Geospatial Data (Edition 1, Version 1.0. – November 2014) |
| Final Products | Develop and review final products requested by client |

## Deliverables

The deliverables provided for Klamath survey project are shown in Table 8. The deliverables are provided electronically and can be found on the portable hard disk accompanying this report.

**Table 8:  Survey Data Deliverables**

| Electronic Data Deliverables | |
|---|---|
| **Point Cloud Data Package** | Point Cloud (*.las) and Tiled<br><br>● Topographic LiDAR Points<br><br>● Bathymetric LiDAR Points<br><br>● Conventional Points (GNSS RTK)<br><br>● Multibeam Sonar (CUBE Algorithm)<br><br>● Sweep Sonar (CUBE Algorithm) |
| **Digital Imagery** | Full Resolution  Data Package<br><br>● Tiled Orthorecitfied Image Mosaics (*.tif)<br><br>● Ground Control (*.shp)<br><br>● Ground Survey Check Points (*.shp)<br><br>● Aircraft Position (*.shp)<br><br>General Use Data Package<br><br>● Orthorectified Image Mosaic (*.sid) |
| **Terrain Surface Data Package** | Surface Nodes Data Package<br><br>● Tiled XYZ Tables of Final Ground Surface Nodes Including Densified Points Derived from Breaklines; ASCII(*.txt)<br><br>Contour Data Package<br><br>● Tiled Seamless Contours (0.5 meter) (*.shp)(*.dxf)<br><br>Breakline Data Package<br><br>● Tiled Seamless Breaklines (*.shp)<br><br>Terrain Model Data Package<br><br>● ArcGIS FileGeodatabase (*.gdb)<br><br>Raster Data Package<br><br>● Half Meter Raster (*.flt) |
| **Terrain Accuracy Data Package** | Ground Survey Check Points (*.xlsx)<br><br>● Absolute Vertical Accuracy Assessment |

# RESULTS AND DISCUSSION

## No Data Areas
Areas where data were not acquired were left in the terrain model. All significant areas where there are no bathymetric data are identified in the "Klamath_NoDataAreas" Polygons feature class included in the electronic deliverables.

## ACCURACY ASSESSMENT
Vertical accuracy assessments are based on the guidelines set forth in the National Standard for Spatial Data Accuracy (NSSDA), (FGDC, 1998) as well as the American Society for Photogrammetry and Remote Sensing (ASPRS, 2014). Absolute accuracy is computed using RMSE statistics in non-vegetated terrain and 95th percentile statistics in vegetated terrain. The aforementioned accuracy standards were developed primarily to describe terrestrial data so it is necessary to extend the meaning of non-vegetated and vegetated when it comes to the bathymetric surface. For the purposes of this accuracy assessment non-vegetated has been extended to include all sonar and conventional survey data collected in relatively flat areas within the wetted channel that contain uniform substrate smaller than the boulder size class and in areas with good water conditions (non-aerated water). Vegetated has been extended to include the remainder of the bathymetric surface; steep slopes non-uniform substrate, boulder and bedrock and aerated water.

### Absolute Vertical Accuracy
For the topo-bathymetric LiDAR and sonar datasets, absolute vertical accuracy was assessed using Non-Vegetated Vertical Accuracy (NVA) Reporting. NVA accuracy reporting compares point data collected in areas with open sky, with non-turbulent water conditions, where bed substrate is relatively uniform, a lack of vegetation exists and on surfaces with slopes (<20°) to the triangulated irregular network (TIN) surface generated by the survey data. NVA replaces what was formerly known as Fundamental Vertical Accuracy (FVA) and is a measure of the vertical accuracy of the survey data and is evaluated at the 95% confidence interval.

#### Topo-Bathymetric LiDAR
GMA and GDS assessed vertical accuracy of the topo-bathymetric LiDAR dataset by collecting 263 independent GSCP's on the topo-LiDAR surface and 4,806 sonar check points on the bathymetric-LiDAR surface. Results are presented in Table 9. An additional 899 sonar check points were collected on the topo-LiDAR surface and are presented for reference (Table 9).

#### Multibeam and Sweep Sonar
GMA and GDS assessed vertical accuracy of the sonar dataset by collecting sonar crosslines across the main scheme data. Crosslines were primarily collected using multibeam sonar with additional cross lines collected using sweep sonar at the J.C. Boyle reservoir. After nadir beams were extracted from the swath data 35,314 sonar check points were used to assess the accuracy of the multibeam surface and 1,995 points were used to assess the accuracy of the sweep surface. Results are presented in Table 10.

**Table 9: Topo-Bathymetric LiDAR Absolute Accuracy (NVA)**

| Topo-Bathymetric LiDAR Absolute Accuracy | | | |
|---|---|---|---|
| | **Topo LiDAR (GSCP)** | **Topo LiDAR (Sonar)** | **Bathymetric LiDAR (Sonar)** |
| **Samples** | 263 points | 899 Points | 4,806 Points |
| **Average** | 0.001 m | 0.000 m | -0.006 m |
| **Median** | 0.002 m | 0.000 m | -0.009 m |
| **RMSE** | 0.035 m | 0.066 m | 0.052 m |
| **Standard Deviation (1σ)** | 0.035 m | 0.071 m | 0.045 m |
| **1.96σ** | 0.055 m | 0.114 m | 0.100 m |
| **NVA (1.96*RMSE)** | 0.069 m | 0.129 m | 0.101 m |

**Table 10: Sonar Absolute Accuracy (NVA)**

| Sonar Absolute Accuracy (NVA) | | |
|---|---|---|
| | **Multibeam Sonar** | **Sweep Sonar** |
| **Samples** | 35,314 Points | 1,995 Points |
| **Average** | -0.017 m | -0.024 m |
| **Median** | -0.016 m | -0.022 m |
| **RMSE** | 0.048 m | 0.070 m |
| **Standard Deviation (1σ)** | 0.045 m | 0.065 m |
| **1.96σ** | 0.095 m | 0.144 m |
| **NVA (1.96*RMSE)** | 0.094 m | 0.136 m |

# REFERENCES

American Society for Photogrammetry and Remote Sensing, ASPRS Positional Accuracy Standards for Digital Geospatial Data. Edition 1, Version 1, November 2014. http://www.asprs.org/PAD-Division/ASPRS-POSITIONAL-ACCURACY-STANDARDS-FOR-DIGITAL-GEOSPATIAL-DATA.htm

Federal Geographic Data Committee, Geospatial Positioning Accuracy Standards (FGDC-STD-007.3-1998).  Part 3:  National Standard for Spatial Data Accuracy. http://www.fgdc.gov/standards/projects/FGDC-standards-projects/accuracy/part3/chapter3

Quantum Spatial Inc. Klamath Reservoirs, California and Oregon, Topobathymetric LiDAR Technical Data Report, October 29, 2018

## APPENDICES

### Appendix A-1: Survey Control Coordinates -- Geographic
### NAD83(2011) Datum, epoch 2010.00

| Monument ID | Latitude (N) | Longitude (W) | Ellipsoid Height (m) | Group | Type | Comment |
|---|---|---|---|---|---|---|
| P380 | 42° 15' 34.79886" | 121° 46' 46.85526" | 1391.280 | QSI | ORGN RTN | |
| KLAM_RTK_01 | 41° 55' 53.60915" | 122° 26' 30.05496" | 644.842 | QSI | Rebar with Cap | |
| DH6397 | N41°53'55.73736" | W122°33'51.85263" | 681.022 | NGS | Survey Disk | Held |
| DF9369 | N42°11'38.78988" | W121°47'14.54849" | 1236.222 | NGS | Survey Disk | Held |
| NZ1016 | N42°06'56.74432" | W122°06'53.47462" | 1391.879 | NGS | Metal Rod | Vertical Check |
| NZ1023 | N42°08'27.91179" | W122°00'43.77427" | 1166.120 | NGS | Metal Rod | Vertical Check |
| GMA-200 | N42°07'21.97179" | W122°02'52.79449" | 1136.533 | GMA | Scribe | Adjusted |
| GMA-201 | N42°05'32.08620" | W122°04'20.86394" | 995.363 | GMA | Rebar with Cap | Adjusted |
| GMA-202 | N41°58'25.76728" | W122°17'55.95491" | 772.760 | GMA | Rebar with Cap | Adjusted |
| GMA-203 | N41°57'50.65426" | W122°25'49.06258" | 731.917 | GMA | Rebar with Cap | Adjusted |
| GMA-205 | N41°55'59.62588" | W122°26'03.25854" | 727.094 | GMA | Rebar with Cap | Adjusted |
| WCP-101 | N41°58'24.42160" | W122°22'02.16531" | 696.489 | Woolpert | Rebar with Cap | Adjusted |
| WCP-102 | N41°57'51.74165" | W122°15'42.08796" | 774.365 | Woolpert | Rebar with Cap | Adjusted |
| WCP-103 | N42°00'14.16431" | W122°11'13.78885" | 852.313 | Woolpert | Rebar with Cap | Adjusted |
| WCP-104 | N42°02'34.29919" | W122°04'53.05303" | 1262.654 | Woolpert | Rebar with Cap | Adjusted |
| KR-IGD_DB4 | N42°05'46.83442" | W122°02'54.77961" | 1246.978 | WSI | Rebar | Adjusted |

**Appendix A-2: Survey Control Coordinates -- Projected**
**NAD83(2011) Datum, epoch 2010.00**
**NAVD88 Datum, Geoid 12B**
**UTM Zone 10, Meters**

| Monument ID | Northing (Meters) | Easting (Meters) | Elevation (Meters) | Group | Type | Comment |
|---|---|---|---|---|---|---|
| P380 | 4679328.224 | 600652.654 | 1413.923 | QSI | ORGN RTN | |
| KLAM_RTK_01 | 4642327.954 | 546288.169 | 668.682 | QSI | Rebar with Cap | |
| DH6397 | 4638633.698 | 536132.198 | 704.790 | NGS | Survey Disk | Held |
| DF9369 | 4672039.878 | 600121.712 | 1259.037 | NGS | Survey Disk | Held |
| NZ1016 | 4663008.377 | 573172.966 | 1415.089 | NGS | Metal Rod | Vertical Check |
| NZ1023 | 4665913.277 | 581630.045 | 1189.209 | NGS | Metal Rod | Vertical Check |
| GMA-200 | 4663845.882 | 578691.141 | 1159.698 | GMA | Scribe | Adjusted |
| GMA-201 | 4660434.504 | 576705.776 | 1018.612 | GMA | Rebar with Cap | Adjusted |
| GMA-202 | 4647107.673 | 558089.338 | 796.372 | GMA | Rebar with Cap | Adjusted |
| GMA-203 | 4645943.979 | 547208.215 | 755.678 | GMA | Rebar with Cap | Adjusted |
| GMA-205 | 4642517.562 | 546904.057 | 750.933 | GMA | Rebar with Cap | Adjusted |
| WCP-101 | 4647022.057 | 552423.239 | 720.177 | Woolpert | Rebar with Cap | Adjusted |
| WCP-102 | 4646084.157 | 561179.265 | 797.900 | Woolpert | Rebar with Cap | Adjusted |
| WCP-103 | 4650532.601 | 567313.273 | 875.803 | Woolpert | Rebar with Cap | Adjusted |
| WCP-104 | 4654943.189 | 576025.236 | 1285.989 | Woolpert | Rebar with Cap | Adjusted |
| KR-IGD_DB4 | 4660911.111 | 578678.238 | 1270.187 | WSI | Rebar | Adjusted |

## Appendix B-1: Equipment Specifications

| GNSS Receiver Specifications | |
|---|---|
| **GNSS Receiver** | Trimble R7, R8 Model 3 & R10 |
| Horizontal Accuracy | ± 0.003 m + 0.5 ppm RMS (Static Mode) |
| | ± 0.008 m + 1 ppm RMS (Kinematic Mode) |
| Vertical Accuracy | ± 0.005 m + 0.5 ppm RMS (Static Mode) |
| | ± 0.015 m + 1 ppm RMS (Kinematic Mode) |
| Initialization time | Typically <10 seconds |
| Communications | 460 MHz Narrow Band |

| Applanix POS/MV Specifications | |
|---|---|
| Position Accuracy | 0.02 - 0.1 m (RTK) |
| Heading Resolution | 0.03° (RTK) Long Baseline PP (0.08° Short Baseline) |
| Pitch/Roll Accuracy | 0.02° Independent on Baseline |
| Heave Accuracy | 5 cm or 5% (2 cm RTK) |

| iWBMSc Wideband Multibeam Sonar Settings and Specifications | |
|---|---|
| Swath Coverage | 7-179° (140° Nominal) |
| Range Resolution | <10 mm (Acoustic) |
| Number of Beams | 256-512 EA & ED |
| Operating Frequency | 400kHz w/ 80kHz Bandwidth (200-700kHz Possible) |
| Depth Range | 0.2-275 m (160 meter typical) |
| Ping Rate | up to 50Hz, Range Dependent |
| Resolution | 0.9° Across Track, 1.9° Along Track @400kHz |

| Reason T20-P Multibeam Sonar Settings and Specifications | |
|---|---|
| Swath Coverage | 140° Equi-Distant 165° Equi-Angle |
| Range Resolution | 6 mm |
| Number of Beams | 256-512 EA & ED |
| Operating Frequency | 400kHz w/ 80kHz Bandwidth (190-420kHz frequency agile) |
| Depth Range | 0.5-250 m (150 meter typical) |
| Ping Rate | up to 50Hz, Range Dependent |
| Resolution | 1° Across Track, 1° Along Track @400kHz |

## Sweep System Sonar Settings and Specifications

| | | |
|---|---|---|
| **Transceiver** | | Ross Labs 875-8 |
| | Output Power | 100 watts (RMS) |
| | Resolution | 0.06 ft. |
| | Pulse Length | 0.1 msec |
| | Ping Rate | 55 msec (18.2 Hz) |
| | Recording Rate | 100 msec (10 Hz) |
| | Minimum Depth | 1.5 ft. below transducer face |
| | Maximum Depth | 151 ft. below transducer face |
| **Transducers** | | Airmar |
| | Frequency | 200 kHz |
| | Spread | 8 degree |
| **Pitch and Roll** | | Honeywell HMR3000 |
| | Accuracy | ±0.4 degrees for Tilt < 20 degrees |
| **Position** | | Trimble SPS852 GNSS Receiver |
| | Update Rate | 1 Hz to 20 Hz |
| | Horizontal Accuracy | 0.03 ft. + 1 ppm RMS (RTK) |
| | Vertical Accuracy | 0.05 ft. + 1 ppm RMS (RTK) |
| **Heading** | | Trimble SPS8552H GNSS Receiver |
| | Update Rate | 1 Hz to 20 Hz |
| | Heading Accuracy | 0.09° RMS (2m Antenna Separation) |